NAVAL POSTGRADUATE SCHOOL

MONTEREY, CALIFORNIA

THESIS

DESIGN METHODOLOGY FOR UNDERSTANDING THE SYMPATHETIC DETONATION CHARACTERISTICS OF INSENSITVE HIGH EXPLOSIVES

by

Dinesh Raghavan

December 2005

Thesis Advisor:	Jose O. Sinibaldi
Co-Advisor:	Ronald E. Brown

Approved for public release, distribution is unlimited.

THIS PAGE INTENTIONALLY LEFT BLANK

REPORT DOCUMENTATION PAGE		*Form Approved OMB No. 0704-0188*
Public reporting burden for this collection of information is estimated to average 1 hour per response, including the time for reviewing instruction, searching existing data sources, gathering and maintaining the data needed, and completing and reviewing the collection of information. Send comments regarding this burden estimate or any other aspect of this collection of information, including suggestions for reducing this burden, to Washington Headquarters Services, Directorate for Information Operations and Reports, 1215 Jefferson Davis Highway, Suite 1204, Arlington, VA 22202-4302, and to the Office of Management and Budget, Paperwork Reduction Project (0704-0188) Washington DC 20503.		

1. AGENCY USE ONLY *(Leave blank)*	2. REPORT DATE December 2005	3. REPORT TYPE AND DATES COVERED Master's Thesis
4. TITLE AND SUBTITLE: Design Methodology for Understanding the Sympathetic Detonation Characteristics of Insensitive High Explosives		**5. FUNDING NUMBERS**
6. AUTHOR(S) Dinesh Raghavan		

7. PERFORMING ORGANIZATION NAME(S) AND ADDRESS(ES) Naval Postgraduate School Monterey, CA 93943-5000	8. PERFORMING ORGANIZATION REPORT NUMBER
9. SPONSORING /MONITORING AGENCY NAME(S) AND ADDRESS(ES) N/A	10. SPONSORING/MONITORING AGENCY REPORT NUMBER

11. SUPPLEMENTARY NOTES The views expressed in this thesis are those of the author and do not reflect the official policy or position of the Department of Defense or the U.S. Government.

12a. DISTRIBUTION / AVAILABILITY STATEMENT Approved for public release, distribution is unlimited.	12b. DISTRIBUTION CODE

13. ABSTRACT (maximum 200 words)

 The understanding of sympathetic detonation of energetic materials is important from the stand point of safety, shelf life, storage requirements and handling. The objective of this thesis is to introduce a methodology to assess performance and sensitivity levels of insensitive munitions to sympathetic detonations. AUTODYN code was utilized to validate the shock sensitivity results for Composition B explosives. Upon code validation, simulations were conducted to evaluate small scale sympathetic detonation via gap tests. Similarly, large scale simulations of sympathetic detonations, reflective of real life scenarios, were performed. The understanding of this analysis offers insights for the testing, design and storage orientation of future energetic materials.

14. SUBJECT TERMS Methodology, Sympathetic Detonation, AUTODYN Code, Composition B, Sensitivity, Gap Test, Safe Separation Distance	15. NUMBER OF PAGES 111
	16. PRICE CODE

17. SECURITY CLASSIFICATION OF REPORT Unclassified	18. SECURITY CLASSIFICATION OF THIS PAGE Unclassified	19. SECURITY CLASSIFICATION OF ABSTRACT Unclassified	20. LIMITATION OF ABSTRACT UL

NSN 7540-01-280-5500

Standard Form 298 (Rev. 2-89)
Prescribed by ANSI Std. 239-18

i

THIS PAGE INTENTIONALLY LEFT BLANK

DESIGN METHODOLOGY FOR UNDERSTANDING THE SYMPATHETIC DETONATION CHARACTERISTICS OF INSENSITVE HIGH EXPLOSIVES

Dinesh Raghavan
Ministry of Defense, Singapore
Bachelor in Mechanical Engineering,
University of Manchester Institute of Science and Technology,
Manchester, United Kingdom, 1996.

Submitted in partial fulfillment of the
requirements for the degree of

**MASTER OF SCIENCE IN ENGINEERING SCIENCE
(MECHANICAL ENGINEERING)**

from the

**NAVAL POSTGRADUATE SCHOOL
December 2005**

Author: Dinesh Raghavan

Approved by: Jose O. Sinibaldi
                 Thesis Advisor

                 Ronald E. Brown
                 Co-Advisor

                 Anthony J. Healey
                 Chairman, Department of Mechanical and
                 Astronautical Engineering

iii

THIS PAGE INTENTIONALLY LEFT BLANK

ABSTRACT

The understanding of sympathetic detonation of energetic materials is important from the stand point of safety, shelf life, storage requirements and handling. The objective of this thesis is to introduce a methodology to assess performance and sensitivity levels of insensitive munitions to sympathetic detonations. AUTODYN code was utilized to validate the shock sensitivity results for Composition B explosives. Upon code validation, simulations were conducted to evaluate small scale sympathetic detonation via gap tests. Similarly, large scale simulations of sympathetic detonations, reflective of real life scenarios, were performed. The understanding of this analysis offers insights for the testing, design and storage orientation of future energetic materials.

v

THIS PAGE INTENTIONALLY LEFT BLANK

TABLE OF CONTENTS

LIST OF FIGURES

THIS PAGE INTENTIONALLY LEFT BLANK

LIST OF TABLES

THIS PAGE INTENTIONALLY LEFT BLANK

ACKNOWLEDGMENTS

THIS PAGE INTENTIONALLY LEFT BLANK

I.   INTRODUCTION

The reduction of the hazards of munitions has been the study of numerous organizations for decades. The main objective of these studies is to reduce the unintentional activation of munitions during production, storage, transportation and handling. The consequences of accidents have been catastrophic and in most cases have resulted to loss of human lives and equipment.

The necessity of an increase in the safety of combat platforms has been illustrated by accidents involving munitions on the US aircraft carriers Forrestal (1967), Enterprise (1969) and Nimitz (1981). The problem is not constrained to within the US as there have been many cases of the unintentional detonation in ammunition depots throughout the world.

These accidents are very often the result of sympathetic detonation in which the inadvertent detonation of a single ammunition would trigger off another and subsequently start a chain reaction. It is in this regard that the understanding of sympathetic detonation of the energetic materials is important from a stand point of safety.

A.   OBJECTIVES

The goal of this thesis is to develop a methodology for the assessment of performance and sensitivity of insensitive high explosive to sympathetic detonation. It is important to understand that the characteristic of the sympathetic detonation on high energetic materials is not only affected by peak pressure but also by the duration of the incident shock pulse.

B.   APPROACH

The card gap test is one of the most major and simple technique to estimate the sensitivity of energetic materials and is incorporated for the numerical analysis. Numerical simulations comprising the explosive compound Composition B and the thermoplastic Plexiglass as the gap material are conducted with the aid of the AUTODYN code. The results are validated with existing experimental results to ascertain the required cell and interaction gap sizes.

The results from the validation exercise are then further expanded to analyze the interaction of Composition B in air with regards to sympathetic detonation. Trials were conducted for various donor sizes to study the characteristics of sympathetic detonation. Subsequently, the simulations were conducted on explosive blocks comparable to those of the 155mm Artillery projectiles. Two orientations, head-on and side-on were modeled and their respective safe separation distances determined.

C.   ACCOMPLISHMENT

The strength and duration of the incident pressure wave were analyzed to be related to the explosive mass of the donor. Increasing the air gap between donor and acceptor reduces the strength of the incident pressure wave. Techniques utilizing the pressure and velocity profiles were used to determine the strength of the incident pressure wave and the occurrence of sympathetic detonation.

The orientation of two adjacent explosive blocks was observed to have a significant impact on the safe separation distance. Simulation results show that the side-on orientation reduces the safe separation distance by 25% when compared to the head-on orientation. Hence, the direction of the traveling detonation wave should be ascertained in order to deduce the best ammunition storage orientation that is both safe and space saving.

The simple model for ideal detonation is introduced and two techniques, chemical structures and thermochemistry, for determining detonation parameters are presented. A methodology was established to understand the likelihood of sympathetic detonation for existing and future explosives. The likelihood of sympathetic detonation is dependent on the incident peak pressure and duration. An increase in the separation distance reduces this incident impulse. However, it was shown that knowledge of the spatial orientation of two adjacent explosive blocks is also necessary for the determination of a safe separation distance.

II.   LITERATURE REVIEW

Existing explosives such as RDX and HMX are very powerful but suffer from a relatively high sensitivity. Several approaches can be adopted to improve the sensitivity of current and future explosive by the use of inert and energetic binders. It has been suggested that amino group insertions into futuristic energetic materials may yield explosives with superior Insensitive Munition (IM) characteristics. [4] The ideal IM explosive is one that will not detonate under any conditions other than its intended mission to destroy a target.

The aim of this section is to review some of the more recently investigated and promising high energy molecules that might be considered for future IM applications. Some typical approaches for improving insensitivity of new IM molecules are outlined in the following paragraph.

A.   EXPLOSIVE DEVELOPMENT FOR INSENSTIVE MUNITIONS

1.   Reduced Sensitivity RDX

Certain manufacturing methods produce a grade of high explosive 1,3,5-trinitro-1,3,5-triazinane (RDX), whose cast cured polymer bound explosive (PBX) formulations are significantly less sensitive to sympathetic detonation than those same formulations containing conventional RDX. This grade of RDX has been referred to as Reduced Sensitivity RDX (RS-RDX).

RS-RDX when compared to the conventional RDX has reduced amounts of HMX (byproduct for RDX production) presence, typically less than 0.5%. In addition to the above, RS-RDX has a higher density thus resulting in its crystals having fewer voids and therefore exhibiting less cavitations when transmitting a shock wave. Hence, the number of hot spots is reduced.

2.   1,1-Diamino-2,2 Dinitroehylene (FOX-7)

FOX-7 is a high explosive with similar performance characteristics as RDX but with better stability to shock, friction and heat. FOI, the Swedish Defense Research Agency, has led most of the characterization work for FOX-7. The detonation velocity of

the explosive at a density of 1.756g/cm^3 and 1.5% wax composition is 8.34km/s. The heat of formation of FOX-7 is -32kcal/mol.[7]

A number of published test have shown FOX-7 to be less sensitive then RDX when subjected to mechanical and thermal stimuli. This may be attributed to the "fish bone" like layered crystal structure of the explosive and/or electron bonding characteristics of the attached amino groups in the molecule which counterbalance the withdrawing characteristics of the attached nitro groups in this ethylenic compound. Stability testing has shown FOX-7 compositions to be stable for long term storage when mixed with common stabilizers. FOX-7 is chemically inert and there has never been any case of incompatibility with regards to its mixing with commonly used in explosive formulations. [7]

3.   2,5-Diamino-3,6-dinitropyrazine (ANPZ-I)

Another energetic compound reported by Philbin, Miller and Coombes whose relatively low sensitivity is attributed to amino group attachments is ANPZ-i. [4] It is also believed that stability of the molecules results from aromaticity. The experimental impact sensitivity value is 83cm which is lower than that of RDX. Li and co-workers estimate the detonation velocity of approximately 8.3km/s, similar to RDX. The density is 1.92grams/cc, which is slightly higher then RDX. [5]

Li and co-workers estimate even higher densities and detonation velocities of similar compounds in the family of polynitropyrazines and their N-oxides, many of which may have higher heats of formation and presumably higher detonation energies based on quantum calculations. [5]

4.   Octanitrocubane

In the early 1980's Everett Gilbert of the U.S. Army Armament Research and Development Command pointed out that the nitrocarbon Octanitrocubane (ONC) has a perfect oxygen balance and should have high heat of formation per CNO_2 unit and exceptionally high density as well.

Both statistical and computational approaches predicted a density of 2.1-2.2g/cm^3 for ONC.[3] Recently published calculated value of heat of formation of solid ONC moved a line of text down for more text at top of page [(CNO$_2$)$_8$] is 594kJ/mol, corresponding to 74kJ/ (CNO$_2$)-mole.[3] The theoretical estimate of the detonation velocity for ONC is 9.9km/s comparable to CL-20 and faster than HMX [3].

Cubane has its skeleton in the shape of a cube. At each corner of this cube there is a carbon atom, carrying a hydrogen, bound to three identical neighboring carbons. The internuclear CCC angles are 90°, far off from the standard 109.5°. Cubane is strained to about 695kJ/mol, corresponding to a substantial weakening of its bonds. The large bond angle of deformation in cubane makes it a power house of stored energy. However, studies done to date show cubane and most of its derivative to be stable. The energy of activation for thermal decomposition of cubane in gas phase is 180kJ/mol at 230-260°C, so the molecule decomposes only slowly at such temperatures.

The density of ONC now in hand is 1.979g/cm^3, still lower than that calculated. However, it is suffice to conclude that ONC exist and is stable. To adopt ONC as an explosive, significant quantities of it must be made for the exploration of its properties prior to its introduction as an explosive.

B.   INSENSITIVE MUNITIONS TESTING

1.   Modeling

The current qualification process for which explosive are accepted as insensitive are based almost solely on testing. However the capabilities of computational modeling have increased and modeling offers the ability to compare different tests and to address a wider range of responses than can be tested through experiment alone.

2.   System Integration

While the development to test and produce insensitive high explosives will continue, there is also a need to understand how an insensitive high explosive is to be qualified as IM. IM is not just a characteristic of the energetic material but it is a synergetic effort of the combination of the energetic material and the end item application. The "IMness" of an energetic material might be defined as the ability of the

material within its system to retain its bonds strength between atoms, molecules or chains when subjected to an unintended external stimulus or by the cumulative environmentally induced stressors throughout its life time.

Therefore, the goal of any good test and evaluation programme is to capture knowledge of those environmental stressors and to deduce the individual and cumulative effects of the stressors. The use of sensors, small scale test methods and in-situ monitoring devices allows for the assessment of the effect of the IM to external and aging related stimuli.

C. CODE VALIDATION

Two valuable inputs for examining shock sensitivity came from a reported study of the Gap Sensitivity Test and the concurrent use of the Century Dynamic, Inc. AUTODYN code by NPS researchers on on-going explosives research.

1. Numerical Gap Test Study

Recently reported numerical investigations of the gap test by Kubota were considered to be a good starting point for this research. The intent of the investigation was to build to demonstrate a technique that would be useful for examining shock sensitivity of explosives much larger in size than can be accommodated by experiment. They used finite difference techniques to simulate experimental data for Composition B. They also correlated their findings to the Popalato run-to-detonation equation. [1]

The experimental and numerical data, parameters for the equation-of-state and detonation burn models from this study, were introduced into this thesis research.

2. Finite Difference Code

The Century Dynamic AUTODYN family of finite difference codes includes a Lagrangian processor. The library files for the code include the same parameters for the JWL equation of state and the Lee-Tarver ignition and growth model that were used by Kubota.

It is important to note that Kubota used an Eulerian finite difference technique, whereas the Lagrangian processor in AUTODYN is used in this study.

III. METHODOLOGY

This section provides the various methodologies available to formulate a basis for evaluating the potential of an explosive. It seeks to introduce the tools available for the estimation of detonation parameters and explosive effects of new explosives. An understanding of detonation theory allows for a more in depth analysis to the physics behind the simulation results.

Quantitative analysis is also dependent on accuracy of the models used to treat the pressure-volume behaviour of the unreacted and reaction products.

A. DETONATION THEORY

The detonation zone is a complicated region. The simple theory or the Zeldovich, Von Neumann and Döering model, which describes the ideal detonation case in a simplified manner, makes a few assumptions that agree with gross observations. [1] These assumptions are:

1. The flow is one dimensional.

2. The front of the detonation is a jump discontinuity.

3. The reaction-product gases leaving the detonation front are in chemical and thermodynamic equilibrium and the chemical reaction is completed.

4. The chemical reaction-zone length is zero.

5. The detonation rate or velocity is constant; this is a steady-state process; the products leaving the detonation remain at the same state independent of time.

6. The gaseous reaction products, after leaving the detonation front, may be time dependent and are affected by the surrounding system or boundary conditions.

With these constrains, the detonation is seen as a shock wave moving through an explosive. The shock front compresses and heats the explosive, which initiates chemical reaction. The exothermic reaction is completed almost instantly. The energy liberated by the reaction feeds the shock front and drives it forward. At the same time the gaseous products behind the shock wave are expanding, a rarefaction wave moves forward into the shock. The shock front, chemical reaction and the leading edge of rarefaction are all in equilibrium; so they are all moving at the shock detonation velocity.
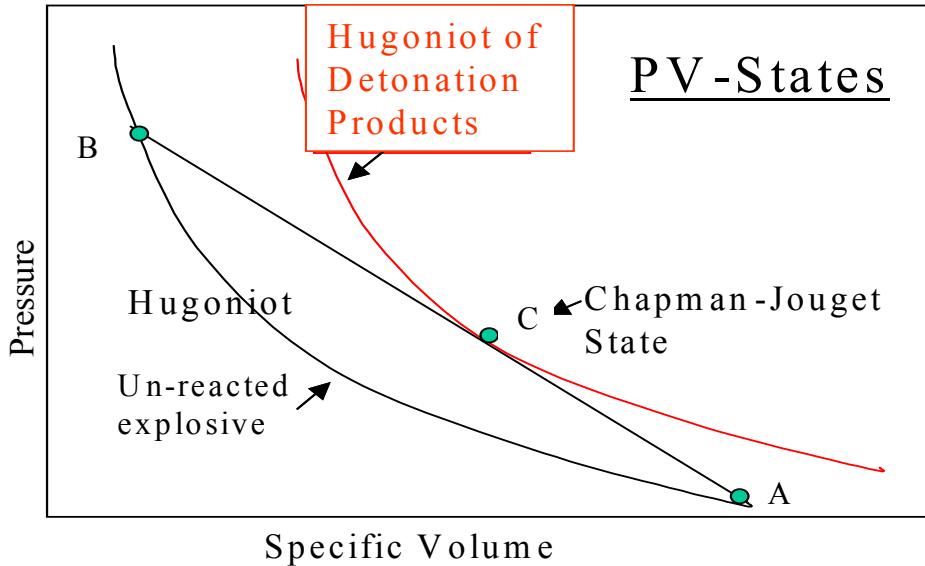
Figure 1.   P-ν Plane Representation of Detonation

With reference to Figure 1, the initial state is at point A for the unreacted explosive. As the explosive is compressed by the shock front it jumps via the unreacted Hugoniot curve to point B (Von Neumann spike), the condition for fully shocked but as yet unreacted explosive. Due to the short reaction zone and fast reaction, the energy involved in this pressure spike is negligible compared to the energy in the fully reacted products. In the simple model, the Von Neumann spike is ignored and the reaction zone thickness is assumed to be zero.

The state of the reaction products is at point C (Chapman-Jouguet point). This is where the Raleigh line is tangent to the product Hugoniot. It is only at this point that the slope of the Hugoniot (products) equals the slope of the Raleigh line thus implying that the reaction zone, rarefaction front and shock front are all traveling at the same velocity.

When an explosive is shocked it does not instantly attain full steady-state detonation. The shock must travel some finite distance into the explosive before steady-state detonation can be achieved. This "run distance" is not a constant, but varies with the peak input shock pressure. The higher the pressure, the shorter the run distance. When the run distance versus input shock pressure data are plotted on a log-log format, the data fall onto approximately straight lines. This data representation is called a "Pop-

plot". From the Pop-plots, we are able to establish equations of input shock pressure as a function of run distance for each explosive tested. [1]

1. The "Shock" Equation of State

Shock waves occur when a material is stressed far beyond its elastic limit by a pressure distribution. As the pressure-wave velocity increases with pressure above the elastic limit, a smooth pressure disturbance "shocks-up." Hence, a shock refers to the discontinuity across a shock front where the original states of particle velocity μ_o, density ρ_0, internal energy E_0, and pressure P_0, suddenly changes across the shock front to particle velocity μ_1, density ρ_1, internal energy E_1, and pressure P_1. They do not change gradually along some gradient or path but discontinuously jump from unshocked to shocked values. As there are five variables, the variable U being the shock velocity, there is thus a need to have five relationships to solve for the variables.

The first three relationships are derived based on the conservation of mass, momentum and energy across the shock front. These relationships are called the "Rankine-Hugoniot jump equations" and they are as follows:

Mass Equation: $\qquad\qquad\qquad \dfrac{\rho_1}{\rho_0} = \dfrac{U}{U-\mu} = \dfrac{v_o}{v_1}$ $\qquad\qquad$ (1)

Momentum Equation: $P_0 - P_1 = \rho_0 \left(\mu_1 - \mu_0 \right)\left(U - \mu_0 \right)$ $\qquad\qquad$ (2)

Energy Equation: $\qquad\qquad E_1 - E_0 = \dfrac{P_1 \mu_1 - P_0 \mu_0}{\rho_0 \left(U - \mu_0 \right)} - \dfrac{1}{2}\left(\mu_1^2 - \mu_0^2 \right)$ $\qquad\qquad$ (3)

The subscripts 0 and 1 refer to the states just in front of and just behind the shock front, respectively.

Many experiments were conducted to determine that the shock velocity is linearly related to the particle velocity, for most material and this relationship is as follows:

a. U-μ Hugoniot Equation: $\quad U = C_0 + s\mu$ $\qquad\qquad\qquad\qquad$ (4)

where C_0 is the bulk sound velocity and the term s is a dimensionless constant. It should be noted that the U-μ equations for materials may also be expressed as U=C_0 + sμ+qμ^2. This relationship was derived from the least-squares fits to the data and q is

9

another dimensionless constant. In this case, the data is composed of two or more straight-line segments with a transition region between them. The reason for the shift in slope of the U-μ Hugoniot is most likely that a phase change or a shift in crystal lattice has occurred at that point.

By combining the U-μ Hugoniot equation with the momentum and mass equation, and let $P_0 = 0$ and $\mu_0 = 0$, thus eliminating the particle and shock velocity terms and arriving to the expression:

P-v Hugoniot Equation: $\qquad P = C_0^2 \left(v_0 - v \right) \left[v_0 - s \left(v_0 - v \right) \right]^{-2}$ $\qquad$ (5)

The Hugoniot is the locus of all possible equilibrium states in which a particular material can exist. Since the Hugoniot represents the locus of all possible states behind the shock front, then a line joining the initial and final states on the P-v Hugoniot represents the jump condition. This line is called the Raleigh line and is given as follows:

Raleigh Equation: $\qquad P_1 - P_0 = \dfrac{U^2}{v_0} - \dfrac{U^2}{v_0^2} v_1$ $\qquad$ (6)

where U is the shock or detonation velocity.

If the final and initial P-v states of a shock are known then the shock or detonation velocity is given by the slope of the Raleigh line ($-\rho_0^2 U^2$). The point where the Raleigh line intersects with the unreacted explosive is the Von Neumann spike.

It is possible to manipulate the U-μ Hugoniot equations with the momentum equations to eliminate U, leaving P-μ relationship:

7. P-μ Hugoniot Equation: $P_1 = \rho_0 \mu_1 \left(C_0 + s \mu_1 \right)$ $\qquad$ (7)

2. Chapman-Jouguet State and Equation of State (EOS)

The final chemical reaction of CHNO explosives during detonation results in the production of molecular nitrogen, oxides of hydrogen and carbon, and residue carbon. The composition of products is partially dependent on the oxygen balance in the explosive molecule. The equilibrium state at which the steady state reaction occurs is defined by the tangency of the Raleigh line, which connects the von Neumann spike along the equation of state (or Hugoniot of the unreacted explosive) and the ambient

specific volume of the explosive, and the equation of state of the highly compressed product gases. This tangent point is referred to as the Chapman-Jouguet (C-J) state. The gas density at this state is approximately 33 percent that of the explosive at ambient condition. Because of the close crowding of the gaseous molecules, the P-ν relationship deviates greatly from ideal gas law. Thus, much different relations must be used to describe pressure-volume expansion and compression about the detonation state condition.

The most common relationship used to describe gaseous behavior about the C-J state is the so-called JWL equation of state which is in the following form,

$$P = A\left(1 - \frac{\omega}{R_1 \xi}\right) e^{-R_1 \xi} + B\left(1 - \frac{\omega}{R_2 \xi}\right) e^{-R_2 \xi} + \frac{\omega}{\xi} E \tag{8}$$

where A, B, E, R_1, R_2 are all constants, ω is the Gruneisen coefficient and $\xi = \frac{\rho_0}{\rho}$, subscript 0 indicates initial state of condensed explosive. R_1, R_2, and ω are dimensionless while A, B, and E have dimensions of pressure.

The parameters of this equation are usually determined by an iterative process using data from a standard experiment referred to as Cylinder Expansion. The coefficients of this equation used to simulate the shock response of Composition B are tabulated in Table 1. These values are identical to those used by the previously cited Kubota report.

Table 1.   JWL Parameters for Composition B from Kubota. [2]

Explosive	Phase	A(GPa)	B(GPa)	R_1	R_2	ω	E(GPa)
Composition B	Reacted	524	7.678	4.2	1.1	0.34	8.5
	Unreacted	788	-5.03	11.3	1.13	0.894	-0.612

It is quite common to use the form of the P-ν equation derived from experimentally determined parameters of the U-μ Hugoniot equation for modeling the behavior of the unreacted explosive at high plastic strain conditions. However, in order to replicate the Kubota results, a form of the JWL equation was used. The JWL parameters for the unreacted explosive are also shown in Table 1. As shown in Figure 2, there are

quite large differences between the P-ν coordinates predicted by two equations: The values used for terms c_o and s in the Hugoniot equation were taken from the previously cited Cooper [1]. The effect of these differences was not treated in this research. They should be investigated in the future.
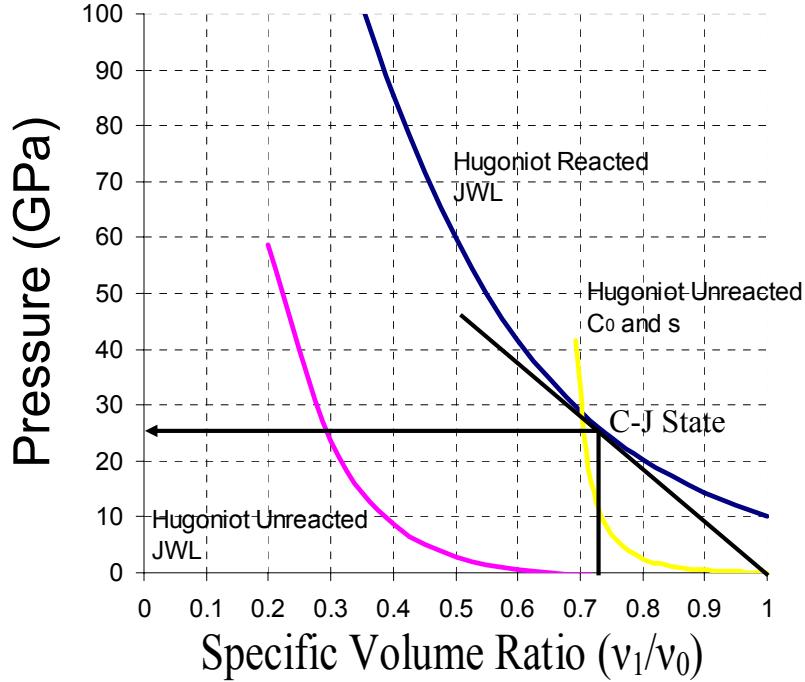
Figure 2.   Unreacted and Reacted Hugoniots for Composition B

3.   Lee-Tarver Ignition and Growth Model

There have been many attempts to characterize hazards associated with explosives. Simple models where the initiation threshold is characterized by values of the impact pressure P and its duration t have been successful in providing criteria for initiation with simple geometries, but they have not been shown to be reliable for more complex problems. Early models such as the Forest Fire model is able to match the Pop plots, but it is not as successful in matching pressure-time data obtained from gauges embedded in the explosive. The Lee Tarver ignition and growth model is able to match gauge data as well as the Pop plots. [14]

The Lee-Tarver model is based on the assumption supported by experimental data that ignition starts at hot spots and grows outwards form these sites. The early models described a two-step reaction rate model with a term for ignition of the explosive and a term for growth. This model was improved to a three-step process comprising ignition, growth and completion. This new model overcame discrepancies observed with the earlier models for very short shock pulse duration initiation data. [14]

The latest Lee Tarver model gives a quick pressure spike on ignition, followed by a slow growth of the reaction that accelerates when the regions around the hot spots begin to coalesce. The Lee-Tarver model is applied to the acceptor.

The Lee-Tarver equation consists of there basic parts:

1.   An equation of state for the inert explosive (a choice between a shock form or a JWL form)

2.   Reaction rate equation to describe ignition, growth and completion of burning

3.   JWL equation of state for the reacted detonation products

The Lee Tarver ignition and growth model is expressed as follows:

$$\frac{d\lambda}{dt} = I(1-\lambda)^{\frac{2}{9}}\eta^4 + G(1-\lambda)^{\frac{2}{9}}\lambda^{\frac{2}{3}}P^z \tag{9}$$

where λ is the mass fraction of detonation products; $\lambda = 0$ corresponds to the unreacted state and $\lambda = 1$ to the completely reacted state, and $\eta = \rho/\rho_0 - 1$. The parameters z, G and I are constants whose value depend on the explosive properties and are chosen as giving the best agreement with shock initiation experimental data.

There is an increasing amount of attention being given towards the development of empirical methods for estimating the parameters of the Lee-Tarver equation by molecular family group. Results of recent IM studies also suggest the effect of grain size and impurities can be modeled by adjusting the z, G and I parameters.

B.   ESTIMATING THE LOCATION OF THE CHAPMAN-JOUGUET STATE AND THE BEHAVIOUR OF DETONATION PRODUCT GASES

As previously addressed, there are at least two often-used models for estimating the effect of high-rate plastic behavior compression of an unreacted explosive: (a) the

Hugoniot equation of state based on parameters from the wave equation and (b) a modified JWL form.

CYLEX-based data (from cylinder expansion) are used to estimate the cumulative equation of states of reaction products in the form of the JWL. The Gurney equation approximation can also be used for determining equation-of state parameters of reaction products. Well-tested approaches for estimating the detonation velocity and pressure at the Chapman-Jouguet state, outlined in the following paragraphs, provide means for predicting these key parameters. These tools are necessary for treating newly synthesized explosives which are in limited supply and envisioned explosives, where the elemental composition or thermochemical characteristics are known, or (b) molecular structures are known.

Basically, an estimate of the ambient density and C-J pressure provides sufficient information to predict detonation velocity. This prediction then offers an opportunity to predict the Gurney constant, and based on work by Miller and Alexander the coefficients of the JWL equation for detonation products.

1. Theoretical Maximum Density (TMD)

Eremenko developed a technique for estimating TMD based on molecular class of organic molecules. He established 13 classes of organic compounds, within which fits most of the conventional explosives known and envisioned. The prediction equations are linear functions of hydrogen atom percentage, with slopes and intercepts unique to each organic class. Descriptive details of the molecular groups and respective parameters are included in explosive literature and books, such as Paul Cooper's book entitled "Explosive Engineering". [1]

2. Detonation Velocity

There are three methods for determining detonation velocity. The Stine and Kamlet-Jacobs methods require elemental formulation and thermochemical data (heat of formation). The Rothstein method requires a determined molecular structure. [1]

3. Detonation Pressure

Kamlet-Jacobs provides means for also predicting detonation pressure, using the same information on elemental formulation and thermochemical data. Detonation

pressure can also be predicted based on the often-used approximation of the ratio of specific heats of gaseous detonation products (i.e., $\gamma \approx 3$). In this case detonation pressure, P_{cj}, is;

$$P_{cj} = \rho D^2 \Big/ (\gamma + 1) \quad \text{from ref [1]} \tag{10}$$

4. C-J State

The Rayleigh line, along which the shock jump occurs and detonation process proceeds, and the C-J state can then be approximated by the above approximation methodologies.

5. JWL Approximation

The next part of the methodology involves the method of modeling the equation of state of detonation products emanating from the steady state detonation condition about the C-J state. The most common models used to estimate this behavior is the JWL derived by Jones, Lee and Walsh of the Lawrence Livermore National Laboratory, and a recent modification made by Baker and Stiel [16].

The six parameters of the JWL equation of state are approximated from a standard test in which the expansion of a copper lined cylinder is measured. It is the normal practice to best fit the parameters of the equation by iterative hydrocode computations. Miller and Alexander show a more direct and more simplified approach for estimating these parameters based on their observation that the Gurney constant can be directly related to internal energy term in JWL and observations by Wilkins that the expansion of detonation products along the C-J isentrope is independent of explosive composition (i.e., pure explosives). With respect to the Gurney constant, it can be approximated directly from detonation velocity (either through experimental measurement or prediction as indicated by the Rothstein, Stine and/or Kamlet-Jacobs methods). Based on the approach suggested by Miller and Alexander it is conceivable that the expansion experiment can be simulated by inputting the Wilkins result with the Becker, Kistiakowsky and Wilson (BKW) equation, below, which takes into account temperature, an averaging approach to the co-volumes of gaseous mixtures, and a volume expansion term.

$$\frac{pv}{RT} = 1 + \frac{\tilde{b}}{v(T+\theta)^\alpha} \exp\left(\frac{\beta\tilde{b}}{v(T+\theta)^\alpha}\right) \cong 1 + \frac{\tilde{b}}{v(T+\theta)^\alpha} + \beta\left(\frac{\tilde{b}}{v(T+\theta)^\alpha}\right)^2 + \frac{\beta^2}{2}\left(\frac{\tilde{b}}{v(T+\theta)^\alpha}\right)^3 + \cdots \quad (11)$$

θ is a temperature constant $\tilde{b}$ is the weighed sum of individual co-volumes of the detonation gases and β is the volume expansion coefficient.

Correlations to the detonation dynamics of explosives of similar molecular and elemental architecture should provide useful interpretive direction towards approaching optimized solution of the JWL parameters.

6. Summary

The prediction methodologies outlined above should be useful inputs in the assessment of the detonation behavior of new (and envisioned explosives), where experimental data is insufficient.

Using these approaches, the final step in the proposed methodology for estimating shock sensitivity, which is the focus of this thesis research, can proceed.

IV   MODEL VALIDATION

Numerical simulations are an excellent means of conducting initial assessments as they avoid the need for experimental set up and the development of safety procedures, both of which are expensive. The objective of the validation exercise is to calibrate the NPS model with experimental data. This would in turn allow for reasonable estimates when analyzing scenarios that are more pertinent to this thesis. The result from Kubota [2] is used to calibrate the NPS model. The numerical simulations for sympathetic detonation in gap test are conducted by AUTODYN's Langrange solver.

A.   AUTODYN

The Century Dynamics AUTODYN family of finite difference codes includes Eulerian and Lagrangian processors (solvers): Both processors were employed during this research. The code is menu-driven and extremely user friendly. The code is also linked to a comprehensive suite of graphic utilities, which facilitate interpretation. As such, it is a valuable asset for graduate research at the Naval Postgraduate School where there is only a 6-12 month window for Master's Degree research projects. With only a week of training most students are able to setup and solve rather complex problems with assistance from instructors on proper material modeling.

B.   LAGRANGE PROCESSOR

A Lagrange coordinate system is ideal for modeling of flow with relatively low distortion and large displacement that occurs at later times and in regions of low to moderate pressure gradients. For Lagrangian calculation, a grid is embedded in the material and distorts with it, the Lagrangian nodes move with the material. With the grid deforming with the material, time histories are easily obtained and material interfaces and geometric boundaries are sharply defined.

The Lee-Tarver model used for the acceptor (within the gap test) is better modeled by the Lagrange solver.

C.   TRANSMIT BOUNDARIES

In order to economize on the problem size it is advantageous for problems which have only outward traveling solutions to limit the size of the grid by the transmit

boundary condition which allows outward traveling waves to pass through it without reflecting energy back into the computational grid. However it should be noted that the condition is only approximate and some reflected wave will be created by the small inaccuracies in the coding. Such waves do not have a significant impact on the computational solutions for this thesis.

D. INTERACTION

In the case of Lagrange-Lagrange interactions a gap size must be specified even though the subgrids are in contact. The gap size must be between 10% and 50% of the smallest interacting face. The interaction option within AUTODYN is able to compute the gap size for the specified subgrids when selected. It is important to note that if the gap size is zero no interaction will exist thus resulting in no reactions between materials.

E. KUBOTA GAP TEST

A two dimensional Eulerian code to estimate to estimate the explosive phenomenon of high energetic materials which include multi-material flow, large material deformation and shock initiation problems was developed. The computational model of the card gap test as shown in Fig 3.
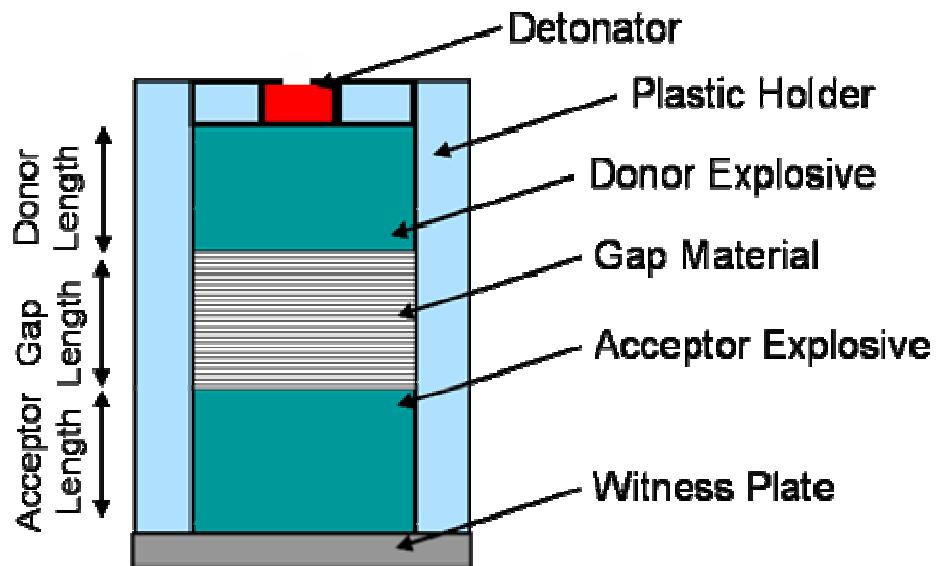

Figure 3.   Computational Model of Card Gap Test

The card gap test is a means to determine the shock sensitivity of an explosive. Both the donor and acceptor charges are Composition B and have cylindrical geometry,

and the gap material is Plexiglas. The dimension of the set up of gap test was varied in this calculation for understanding the effect of size in the gap test. The ratio of length and diameter of both charges is set to 1 and size of charge diameters are varied, 20, 32, 64,126 and 260mm. The detonator, Composition B explosives and Plexiglas gap material were all housed within a Plastic (Plexiglas) holder. The witness plate at the end of the acceptor serves the purpose for identifying detonation within the acceptor. Upon acceptor detonation, the plate if thin enough should disintegrate.

The reaction rate model is used to estimate the degree of decomposition of energetic material via the ignition and growth model. In order to calculate the pressure of reacting explosive, the simple mixture theory, in which the reacting explosive is regarded to be a simple mixture phase of reactant and product components, has been adopted. For the unreacted and reacted phases, JWL equation of state is employed. For Plexiglas the Hugoniot Mie Gruneisen form equation of state is employed.

1.   Experimental Results

The results that were subsequently used for code validation in this thesis are shown in Table 3.

Table 2.   Kubota Test Results [2]

Donor Length (mm)	Gap Length (mm)	Acceptor Length (mm)	Run Distance (mm)
32	15	32	10
32	20	32	25
32	25	32	32

When an explosive is shocked, it does not instantly attain a fully developed steady-state detonation. The shock must travel some finite distance into the explosive before steady-state detonation can be achieved. The higher the pressure, the shorter the run distance. As clearly evident from Table 2, for the minimum gap size the run distance is the shortest indicating high peak input shock pressure.

2.   Experimental Uncertainties

In the experiment by Kubota, no mention was given on the strength of the detonation pulse which initiated the donor and its subsequent impact on the results. In addition to this, both the donor and acceptor were confined in the plastic holder material. The effect of confining the explosive within the material may be minimal but can be

significant at small diameters. At 32mm diameters, the energy loss to the side of the column is large relative to the energy generated at the wave front.

F.   NPS GAP TEST SIMULATION

The NPS gap test is designed to determine the relative shock sensitivity of the explosive. The test also allows for the assessment of run distance. Figure 4 shows the set up for the NPS gap test simulations.
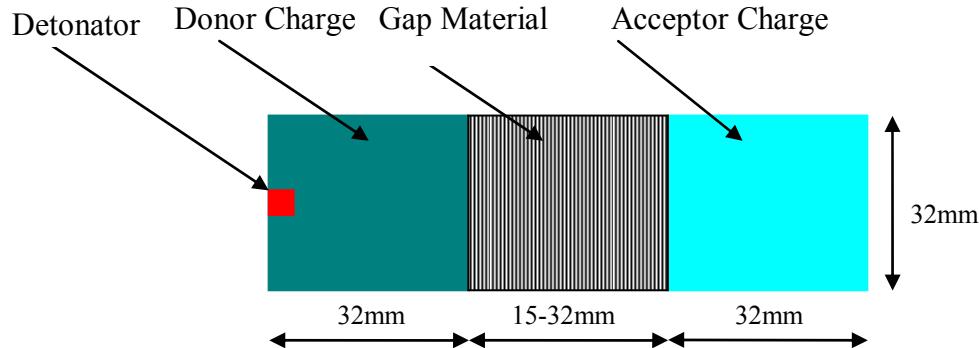
Figure 4.   Gap Test Set Up

The gap test essentially comprises the detonator, donor charge, gap material and acceptor charge. The material properties for each of the component are given in Table 3[1].

Table 3.   NPS Gap Test Material Properties

Component	Material	Density (g/cm^3)	Equation of State	Growth Model	Strength Model
Donor Charge	Composition B	1.717	JWL	None	None
Gap Material	Plexiglas	1.186	Shock	None	None
Acceptor Charge	Composition B JJ3	1.717	JWL	Lee Tarver	Von Mises
Acceptor Charge	Teflon	2.153	Shock	None	None

The Lee Tarver ignition and growth model is used for the acceptor as it is able to match the gauge data as well as the Pop plots. The Composition B JJ3 is an explosive material available in the AUTODYN material library that employs the use of the JWL EOS and the Lee Tarver ignition and growth model. However, repeated trials utilizing Composition B JJ3 acceptor at very fine cell size resulted to Lee Tarver errors during simulations. In an attempt to analyze the cause for these errors, Teflon was chosen to replace for the acceptor material as it is a synthetic material with approximately similar impedance to those of Composition B JJ3.

[1] Values for the EOS and Model parameters used in these simulations are reported in Appendix F.

Subsequent trials conducted with Teflon revealed high pressures at the interface between gap material and the acceptor. The high interface pressure is not possible as Teflon being an inert material is not supposed to increase further the incident shock pulse. This problem was highlighted to Century Dynamics and upon assessment, it was realized that the interaction gap between the components were not specified. The Lagrange code within AUTODYN requires the need to specify the interaction gap size between the donor/gap and gap/acceptor interfaces. This gap size must between 10 and 50% of the smallest interacting surfaces.

1. Model Validation with Teflon Acceptor

The zoning trials were conducted to determine the cell size which best describes the initiation characteristics of the Composition B explosive. In the zoning trials, the Composition B explosive is utilized for the donor charges, Plexiglas for the gap material and Teflon for the acceptor charge. At this point in time, we used a Teflon acceptor as the issue of Lee Tarver errors (described earlier) were concurrently being investigated with Century Dynamics Inc. Analyses were on-going to see if it was only the interaction gap size which was causing the Lee Tarver errors when using the Composition B JJ3 acceptor.

In the first three tests as shown in Table 4, the size of the donor, gap and acceptor were kept constant. The only changes made were the material cell sizes and the interaction gap size.

Table 4.   Zoning Trial with Teflon

Test	Donor Comp B size (mm)	Gap Plexiglas size (mm)	Accept Teflon size (mm)	Donor Cell Size (mm)	Gap Cell Size (mm)	Accept Cell Size (mm)	Interact Gap Size (mm)	Gap/Accept Pressure (GPa)
1	32	24	24	1	0.25	0.25	0.025	7.25
2	32	24	24	1	0.5	0.5	0.05	6.91
3	32	24	24	1	1	1	0.1	6.58
4	32	15	15	1	1	1	0.1	9.84
5	32	15	15	1	2	2	0.2	8.62

Clearly evident from the results is the fact that the gap/acceptor interface pressures decrease as the cell size is increased. This may be explained by the fact that the

interaction gap size is increased as the cell size is increased thus resulting to a lower gap/interface interface pressure. The zoning trial results also show that the gap/interface pressure reduces to estimated levels (6GPa from Kubota [2]) when the cell size is 1mm.

Based on these results, Test 4 and 5 were done to simulate a gap size of 15mm. The gap/acceptor interface pressure reported in Kubota [2] for this gap size with Composition B JJ3 as the acceptor charge is approximately 6GPa. Choosing a cell size of 2mm reduces the gap/interface pressure to 8.62GPa. Hence, at this point we decided that a cell size of 2mm provides for a reasonable initial estimate of the detonation characteristics.

2. Model Validation with Composition B Acceptor

Having estimated an initial cell size of 2mm, the gap test was set up with Composition B JJ3 in the acceptor, similar to Kubota's card gap test. The initial cell size of 2mm was based from the simulation results using the Teflon acceptor. As Teflon and Composition B JJ3 have approximately similar impedances, it was perceived that a 2mm cell size would be a good initial estimate for calibrating Composition B JJ3 explosive. With a gap size of 15mm, the expected interface pressure between the gap and acceptor as reported in Kubota [2] is 6GPa. The dimensions of the donor, gap and acceptor are as follows;

1. Donor: Composition B, Diameter 32mm, Length 32mm
2. Gap: Plexiglass, Diameter 32mm, Length 15mm
3. Acceptor: Composition B JJ3, Diameter 32mm, Length 32mm

Table 5 shows the various simulations conducted.

Table 5. Zoning Trial with Composition B Acceptor

Cell Size (mm)	Interaction Donor/Gap(mm)	Interaction Gap/Acceptor (mm)	Simulation Int Press (GPa)	Kubota Int Press (GPa)
2	0.2	0.2	8.7	6
4	0.4	0.4	8.2	6
4	0.8	0.8	7.4	6
4	1.2	1.2	5.7	6
4	1.2	0.8	6.94	6

Clearly evident from Table 5, is that the interface pressure between the gap and acceptor is approximately 6GPa for a cell size of 4mm and interaction gap size of 1.2mm.

The run distance based on the simulation results is approximately 16mm. It should be pointed out at this juncture the run distance is based on the peak pressure within the acceptor achieving and continuing at approximately 22GPa as shown in Figure 5.

The run distant result is fairly close with the least square fits for shock initiation of 13 mm, for an interface pressure of 5.7GPa. The run distance for the Kubota results (15mm Plexiglas gap length) is 10mm.

As a comparison, Figure 6 shows the case of a 32mm Plexiglas gap where no sympathetic detonation occurred.
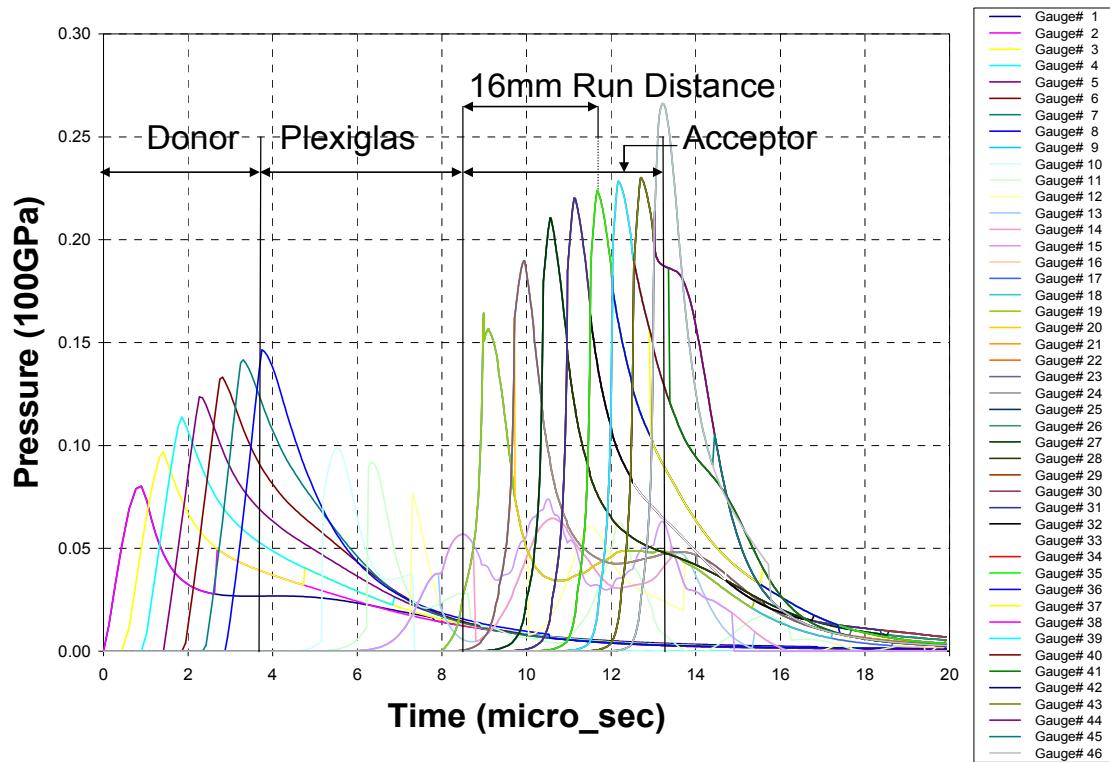

Figure 5.   15mm Plexiglass Gap Showing Sympathetic Detonation
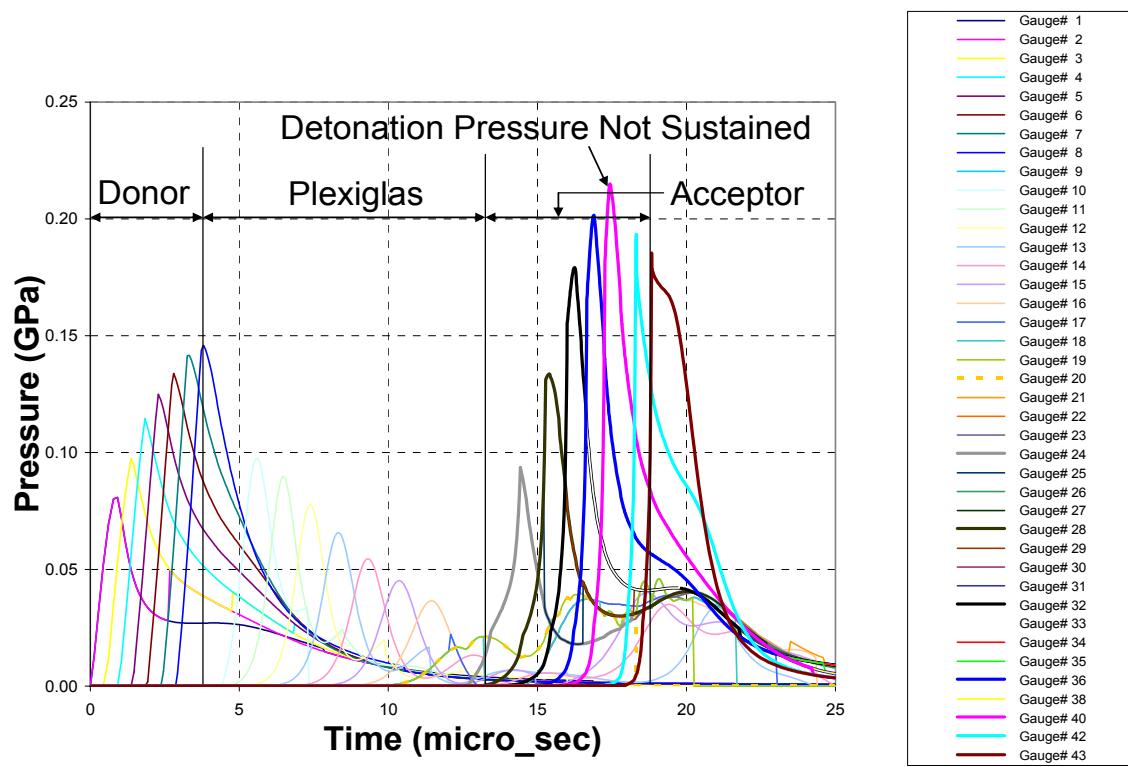
Figure 6.   32mm Plexiglas Gap Showing No Sympathetic Detonation

The "Pop plot" for Composition B based on the least squares fit is presented in Figure 7. The "Pop plot" is a log-log plot between run distance (y-axis) and input shock pressure (x-axis). From the Pop plots, it is possible to establish equations of input shock pressure as a function of run distance. The equation for Composition B is as follows;

$$\text{Log P} = 1.5587 - 0.7164 \log x \text{ from ref [1]}$$

P is the interface pressure and x the run distance.

However, it should be noted that the least square fits for Composition B is only valid for an interface pressure greater than 3.7GPa and lower than 12.6GPa. Hence, in the case of the 32mm Plexiglass gap the interface pressure is 2.12GPa, thus making approximation of run distance by least squares technique questionable.

Although the interface pressure for the 20mm Plexiglass gap length is 3.42GPa (8%lower than 3.7GPa), the least squares estimate is used to determine the run distance, as difference in pressure is minimal and also the technique is only meant to give a reasonable estimate.
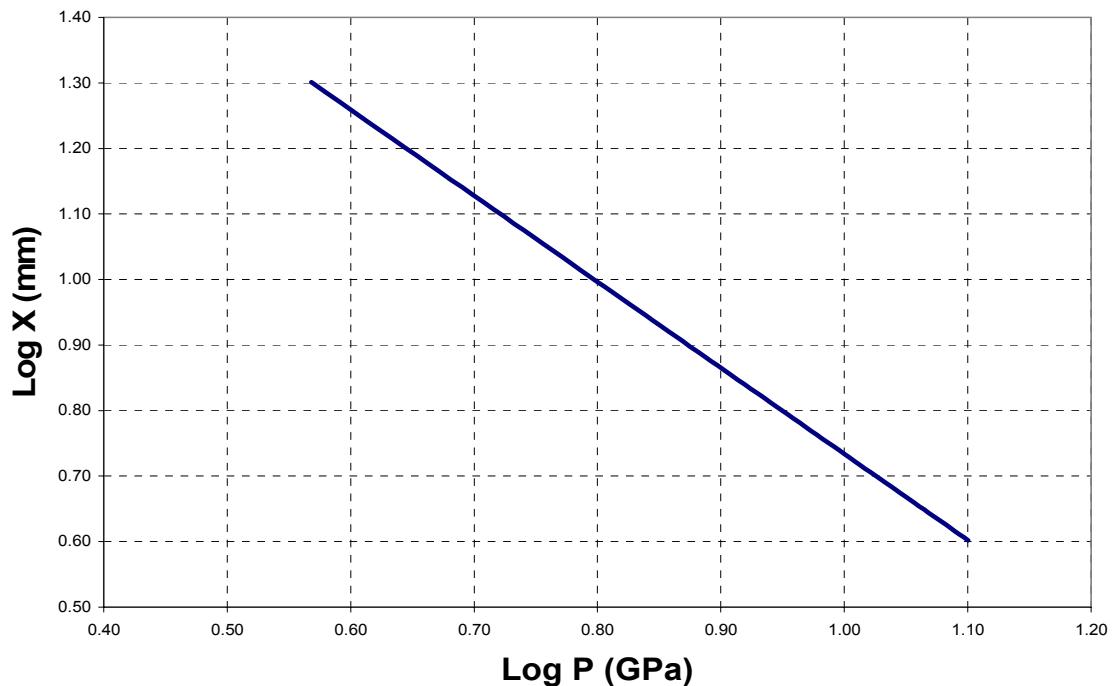

Figure 7.   Pop Plot for Composition B from ref [1]

Taking reference to [1], the detonation velocity and pressure of Composition B at a density of 1.717g/cm^3 are 7.985km/s and 29.04GPa. Figure 8 shows the peak pressure time against gauge location for the 15mm Plexiglas gap.

The average detonation velocities in the donor and acceptor charges are 7.82km/s and 7.19km/s. Based on the expression earlier described for estimating detonation pressures, a density of 1.717g/cm^3 produces detonation pressures of 26.2GPa and 22.2GPa in the donor and acceptor charges respectively.

The average detonation velocity in the donor charge (7.82km/s) is slightly lower than the expected detonation velocity (7.985km/s). After passing through the Plexiglas gap the pressure wave velocity at the leading edge of the acceptor charge is low. This results to a lower (compared to the donor charge) average detonation velocity in the acceptor charge. Hence, this drop in velocity resulted to a drop in the detonation pressure within the acceptor charge (22.2GPa).
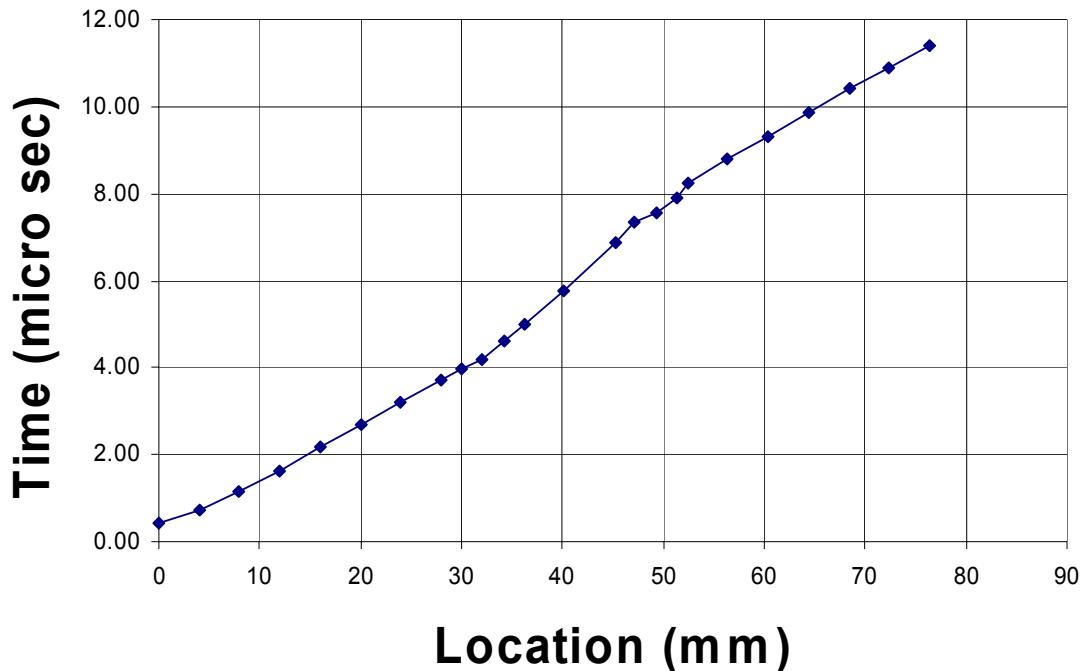

Figure 8.   Distance Time Plot for 15mm Plexiglas Gap

Table 6. Comparison of Simulation Results for Model Validation

| Test No | Gap Size (mm) | NPS Simulations | | | | Kubota | Least Squares |
		Interface Pressure (GPa)	Donor Ave Vel (km/s)	Accept Ave Vel (km/s)	Run Distance (mm)	Run Distance (mm)	Run Distance (mm)
1	15	5.7	7.82	7.19	16	10	12.29
2	20	3.42	7.78	6.56	22	>25	27
3	32	2.12	7.88	5.87	>32	>32	N.A

Table 6 also shows the case when the Plexiglas gap length was increased to 20mm. From the simulation results, the increased Plexiglass gap length reduced the interface pressure (gap/acceptor) to 3.42GPa. The average pressure wave velocity in the acceptor charge is 6.56km/s. The lower interface pressure (compared to 5.7GPa for 15mm Plexiglas gap), reduces the initial pressure wave velocity at the acceptor leading edge which subsequently resulted to a lower acceptor average velocity and a longer run distance, for this case 22mm. Kubota did not state the interface pressure for this scenario but mentioned that the run distance was more than 25mm. Based on the least squares fit, for an interface pressure of 3.42GPa, the run distance is 27mm. The simulations seemed to give fairly reasonable results.

For the last trial, the gap length was increased to 32mm. The simulations results showed the interface pressure (gap/acceptor) to be at 2.12GPa. The average pressure wave velocity in the acceptor charge is 5.87km/s. It should be pointed out that the pressure wave velocity in the acceptor charge was not able to maintain at detonation velocities within the acceptor. The same could be said for the detonation pressure. Although the peak pressure within the acceptor charge reached 22GPa, this pressure was not sustained within the acceptor charge. Figure 9, shows the results of the 32mm Plexiglas gap, the case where no sympathetic detonation is observed. This result is consistent with Kubota.
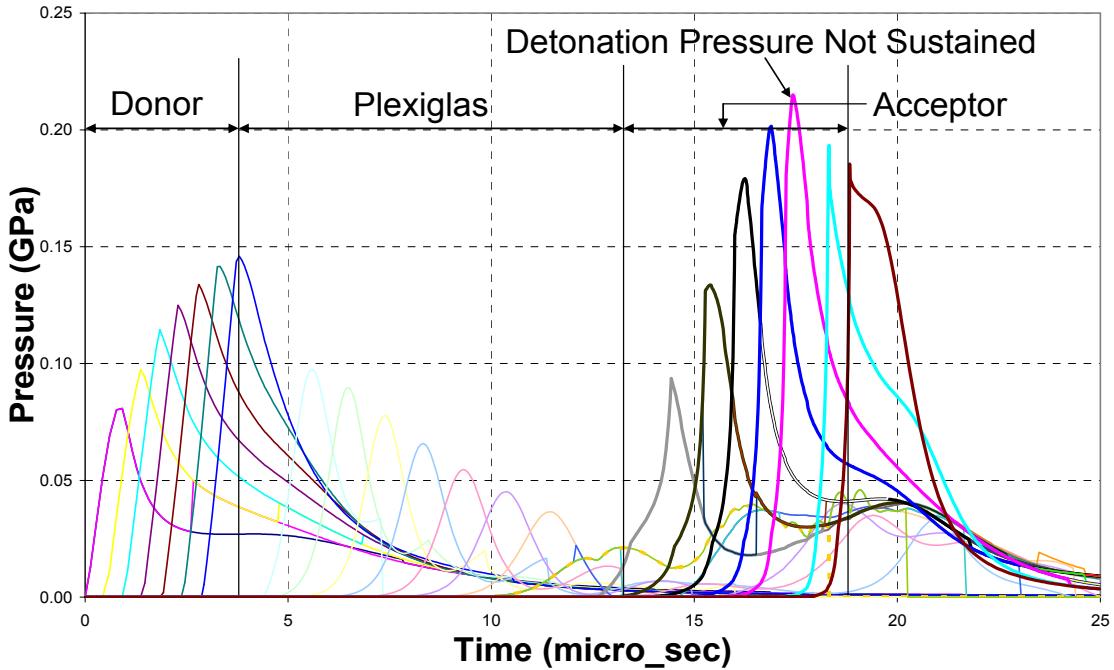
Figure 9.   32mm Plexiglas Gap Length showing No Sympathetic Detonation

3.   Discussion

Table 6 is a comparison of the simulation results between the NPS simulations, Kubota's simulations and the Least Square Fits for shock initiation. Based on these results, it is reasonable to conclude that, a cell size of 4mm coupled with an interaction gap size of 1.2mm, best describes the detonation characteristics of Composition B. Appendix A shows the pressure traces against time for the NPS calibration simulations.

In all cases it is observed that the average detonation velocity in the donor charge is slightly lower than the expected theoretical detonation velocity of 7.985km/s for Composition B. This may be attributed to the gradual built up of the velocities from initiation to full detonation. The average pressure wave velocities within the acceptor charge are lower then the donor in all three tests. This is due to the low pressure wave velocity at the leading edge of the acceptor charge. Also a lower incident pressure would require a longer run distance thus implying a more gradual built up to detonation velocity.

It is also possible that the JWL equation parameters used by Kubota and this research for modeling unreacted Composition B compression are in errors as previously noted.

THIS PAGE INTENTIONALLY LEFT BLANK

V. ANALYSING SYMPATHETIC DETONATION

The validation exercise has determined the cell and interaction gap sizes that best describes the detonation behaviour of Composition B. However, prior to moving into large scale simulations it is worth while to first study sympathetic detonation on a small scale. Small scale analysis in two dimensional axial symmetric modeling would reduce computation times and allow for quick assessment. The emphasis of the small scale analysis is to study the effects of donor sizing on sympathetic detonation.

A. SMALL SCALE SYMPATHETIC DETONATION FOR ANALYSING DONOR SIZING EFFECTS

In the small scale analysis, the donor and acceptor charges used were Composition B, and the gap material used was air. Air gap was chosen in this analysis as it is more reflective of conditions in most ammunition storage facilities. The characteristics of sympathetic detonation are dependent on both the interface peak pressure and duration. The effect of peak pressure has been demonstrated in the validation exercise. In essence, a longer Plexiglass gap length would reduce the incident pressure which in turn leads to a longer run distance and if the incidence pressure is low enough may not result to a sympathetic detonation.

To study the effects of duration of the incident pressure the donor length is varied whilst the gap length and acceptor length are kept constant. The donor has a constant diameter of 32mm but had its length varied from 32mm to 64mm. The air gap and acceptor had their diameters fixed at 32mm and also had fixed lengths of 60mm and 32mm respectively. Figure 10 provides a schematic of the small scale sympathetic detonation set up.

Pressure gauges were placed at 4mm intervals along the central axis of the
donor and acceptor charges
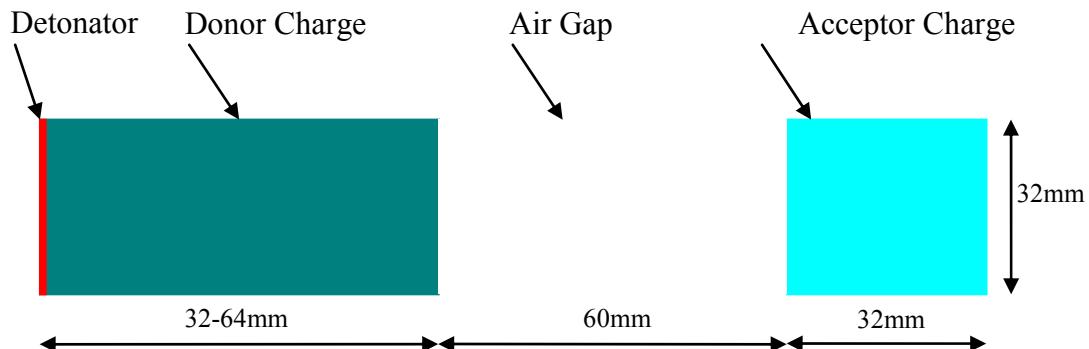
Figure 10.   Small Scale Sympathetic Detonation

In this small scale analysis, a line detonation is used. This is to simulate a planar
detonation wave traveling through the materials. Pressure gauges were placed centrally
along the donor and acceptor charges at 4mm intervals. There were no gauges placed
within the air gap because gauges placed within the air gap did not track the traveling
pressure wave[2].

1.   Analysis of Small Scale Test Results

The first test conducted was on a 32mm length donor charge. The simulation
results depicting the pressure pulses along the donor and acceptor charges are shown in
Figure 11.

---

[2] The gauge locations are provided in Appendix B.
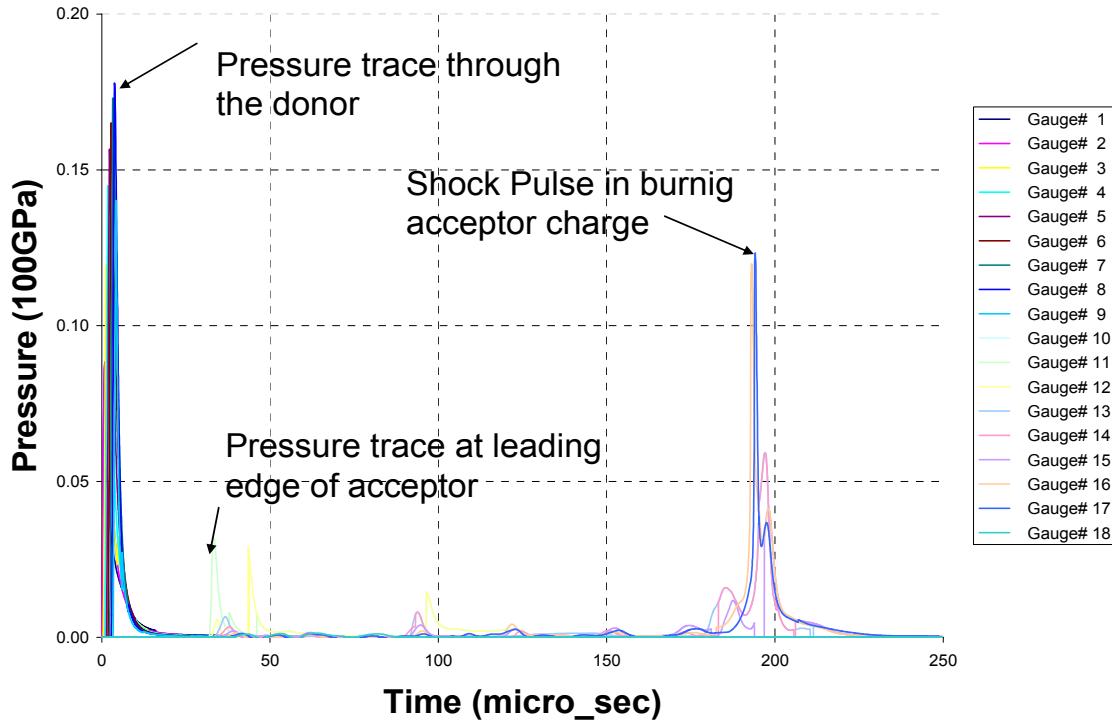
Figure 11.   Pressure Trace for 32mm Donor Charge

As can be seen from Figure 11, the detonation of the donor charge occurs instantly. The pressure at the leading edge of the acceptor charge was approximately at 3.13GPa. The low pressure and duration of the incident pressure wave was not able to initiate sympathetic detonation into the acceptor charge.
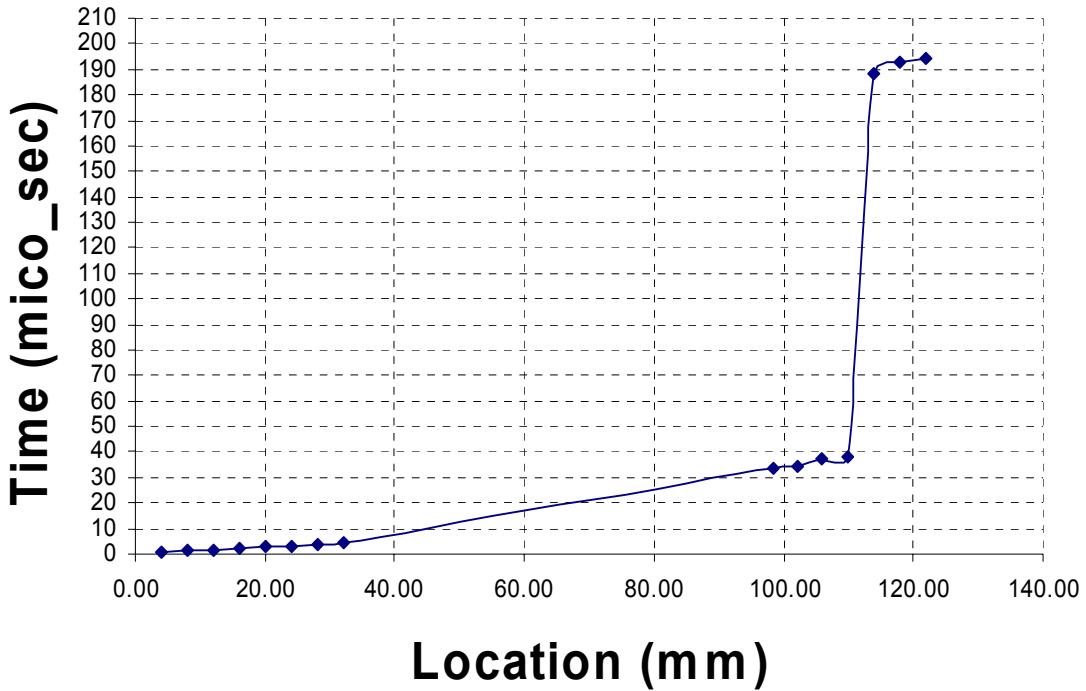
Figure 12.   Distance Time Trace for 32mm Donor Charge

Figure 12 suggest that the incident pressure wave subjected the acceptor charge to burning since the average pressure wave velocity within the acceptor charge is 2.19km/s. The burning of the acceptor charge continued for approximately $150\,\mu$s and then caused a sudden pressure spike (12GPa). However, this shock was not able to detonate the acceptor probably because most of the charge at this time has completed burning.

This same phenomenon was observed for the case when the donor charge length was increased to 48mm.[3] However in the case of the 48mm donor charge, the pressure at the leading edge of the acceptor charge was approximately 3.4GPa (indicating a slightly higher incident pressure wave than for the case of 32mm) and the burning within the acceptor resulted to a higher shock pulse (20GPa) at approximately $270\,\mu$s.

---

[3] The pressure traces for the 48 mm donor charge are provided in Appendix B.

In the third test, the length of the donor charge was increased to 50mm. In this test, as shown in Figure 13, the incident pressure wave was sufficient to initiate a sympathetic detonation at the acceptor charge.
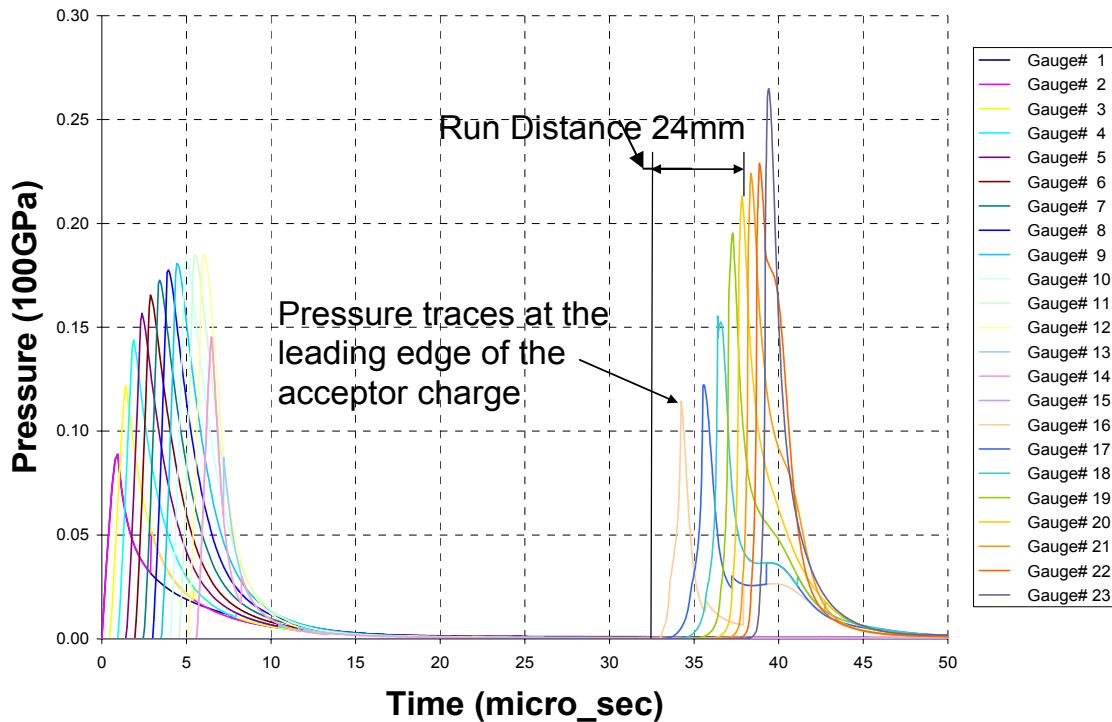
Figure 13.   Pressure Trace for 50mm Donor Charge

Clearly evident from the Figure 13 is that the increased length in the donor charge resulted to a higher incident pressure wave which subsequently increased the leading edge pressure at the acceptor charge. The pressure at the leading edge of the acceptor charge is approximately 11.5GPa. After a run distance of 24mm, the acceptor charge detonated. A run distance of 24mm corresponds to an pressure wave of 3.71GPa according to the least squares fits for shock initiation.
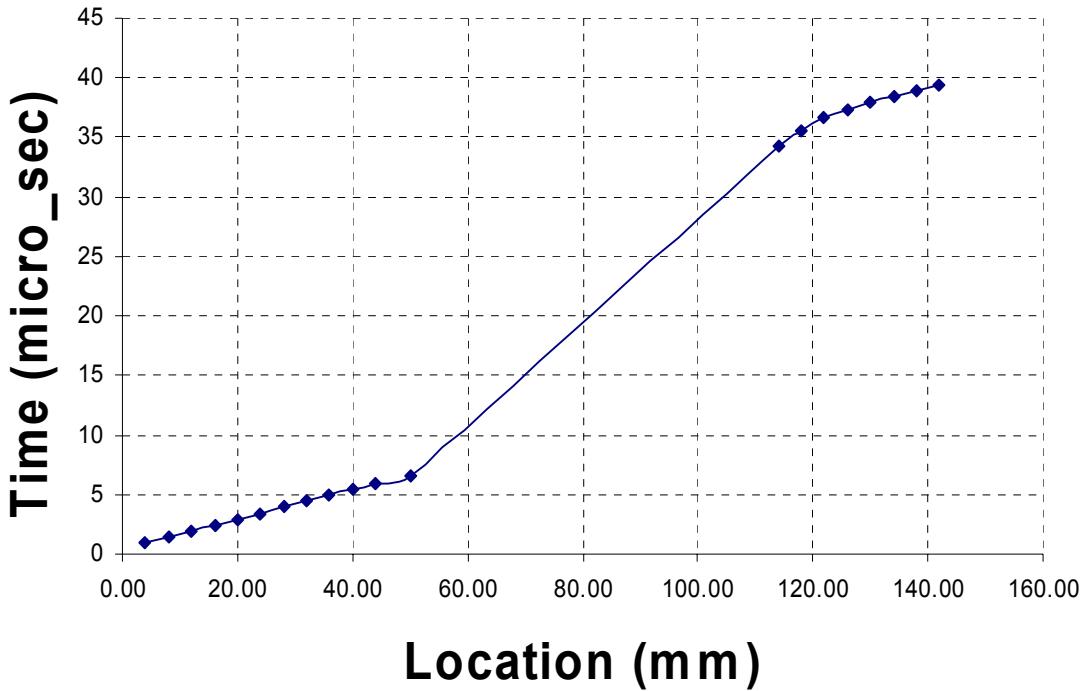
Figure 14.   Distance Time Trace for 50mm Donor Charge

Figure 14 shows the time location trace for the case of the 50mm donor charge. The wave velocity in the acceptor charge gradually increases to 8km/s at approximately 24mm into the acceptor charge. This is consistent with the approximated run distance mentioned earlier. Increasing the donor charges from 50mm to 64mm revealed almost identical characteristics[4].

It should be noted that for the case of the sympathetic detonation the entire sequence from initiation of the donor charge to the complete detonation of the acceptor charge took place within 50µs. This time is very much shorter than the earlier cases where there was no sympathetic detonation and only burning took place within the acceptor charge.

2.   Insights from Small Scale Simulations

The small scale test has revealed that a high incident pressure wave and duration to the acceptor would cause sympathetic detonation. The incident pressure wave and

[4] The pressure traces up to 64 mm donor charge are provided in Appendix B.

duration is directly related to the quantity (mass) of the donor. As apparent from Figure 15 is the fact that a higher donor mass would cause sympathetic detonation. Hence, a higher mass would require a higher gap distance for the avoidance of sympathetic detonation. Figure 15 also shows that the threshold for sympathetic detonation is between donor lengths of 48mm to 50mm. It should be highlighted that because the Go/No Go plots were based on simulation results, the effects of probability (as in a real test) was not considered.
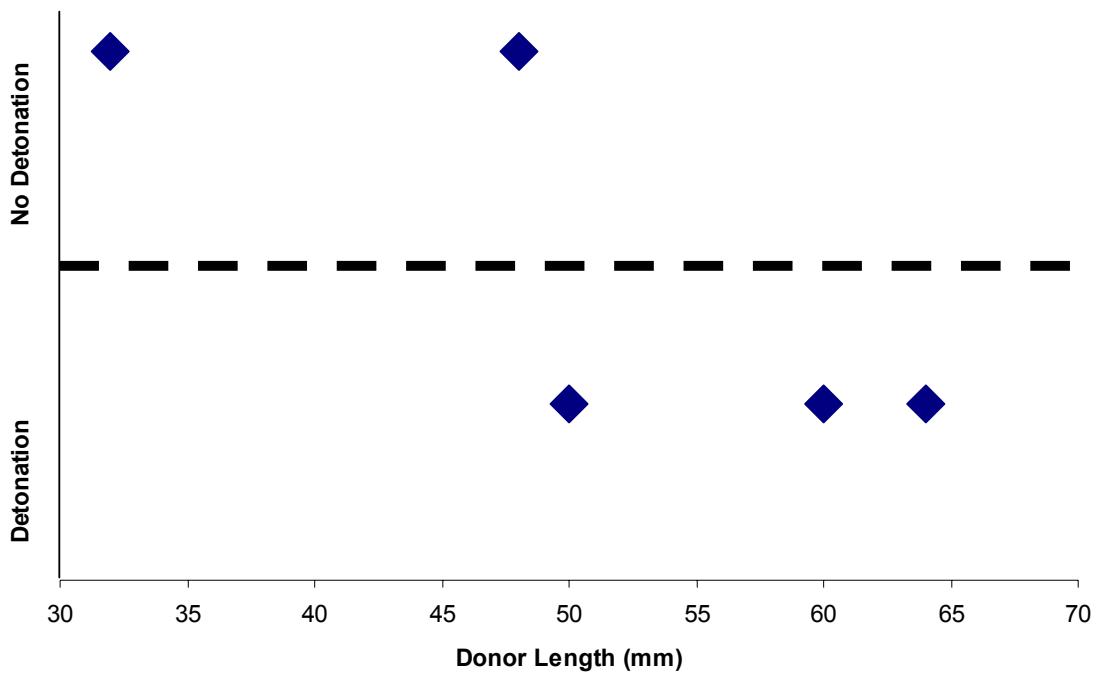
Figure 15.   Go/No Go Small Scale Simulations

From the validation exercise it was determined that a high incident peak pressure would increase the likelihood of sympathetic detonation. However, the small scale sympathetic detonation simulations also revealed that a higher donor mass would increase the duration of the incident impulse thus increasing the likelihood of sympathetic detonation. Hence, it can be concluded that the incident impulse is directly related to the donor mass. An alternative for mitigating the sympathetic detonation effect is increasing the gap length between two adjacent explosive charges.

However at this point it is necessary to introduce the relationship between blast overpressure, distance and donor mass as described in Coopers Explosive Engineers [1] is of the following form;

$$\left(\frac{P^0}{P_a}\right) = f\left[R / \left(\frac{WT_a}{P_a}\right)^{\frac{1}{3}} \right]$$
(12)

where P^0 is the blast overpressure, P_a the ambient pressure, R is the distance from the explosive, W the explosive mass and T_a the ambient temperature. The expression suggests that $R \propto (W)^{1/3}$ which is an important feature to realize when determining safe separation distance.

Consider our test results;

Table 7.   Small Scale Test Results

Donor Length (mm)	Donor Mass (g)	(Donor Mass)$^{1/3}$	Go/No Go	R_{factor}
32	44	3.5	No	No need to increase separation distance
48	66	4.0	No	
50	69	4.1	Go	1.025
60	82	4.3	Go	1.075
64	88	4.4	Go	1.100

At donor length 50mm and above the acceptor charge detonated which suggest the need to increase the air gap length. Based on Table 7, for (Donor Mass)$^{1/3}$ <4.0, the acceptor charge did not detonate. Hence, as a first approximation on the required increase in air gap for donor length of 50mm and above, an R_{factor} is calculated.

The R_{factor} is calculated based on the ratio Donor Mass$^{1/3}$ (detonated) to Donor Mass$^{1/3}$ (not detonated). Donor Mass$^{1/3}$ (not detonated) from Table 7 is 4.0. Hence to have no detonation in the acceptor charges for a donor length of 50mm, 60mm and 64mm it is approximated that their air gap be increased by a factor of 1.025, 1.075 and 1.1 respectively. It should be stressed that this is just an initial approximation and more simulations must be carried out to ascertain the validity of this approximation.

B.   LARGE SCALE SYMPATHETIC DETONATION

As learned from the small scale test, the quantity of explosive has a direct impact on the minimum separation distance (gap) between explosive blocks.   In realistic scenarios, sympathetic detonation usually happens in explosive storage facilities comprising large masses of explosives.   This large scale test will analyze the explosive interaction between two typical artillery projectiles that may be stored within such a facility.   It should be pointed out that this initial analysis does not consider the effects of fragmentation.

Consider a 155mm projectile with its cylindrical cavity measuring 520mm in length and 136mm in diameter, filled Composition B (13kg).   Two orientations, the head-on and side-on are studied in the large scale analysis.   The head-on orientation is where the central axes of both projectiles are in line and the side-on orientation is when the axes are in parallel.

1.   Head-On Simulations

The set up for the head-on simulation is shown in Figure 16.   The pressure gauges are placed along the central longitudinal axis of the Composition B explosives at 40mm intervals (gauges 1 to 28).[5]   Difficulty was experienced in attempts to register pressure pulses in the air gap between explosives.   This is caused either by a deficiency in the code or error in the set up.

The air gap between the two explosive blocks is increased to ascertain the minimum gap required to prevent sympathetic detonation.   All other dimensions within the set up were not altered.   The explosive is initiated at one end (gauge 1) by means of a planar wave detonator thereby propagating the pressure wave through the explosives as depicted in Figure 16.

---

[5] Gauge locations are presented in Appendix C
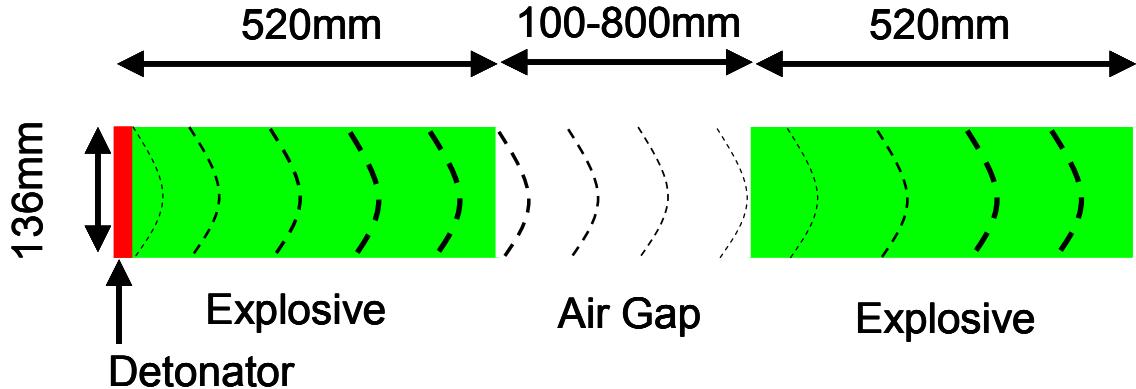
Figure 16.   Head-On Simulation Set Up

a.   *100mm Air Gap*

The first simulation conducted was for a gap distance of 100mm and Figure 17 shows the resulting pressure time graph after $200\,\mu$s. For simplicity only the pressure readings of gauges 20, 24 and 28 of the second explosive are shown as the other gauges show similar characteristics. There is a significant drop in pressure at gauge 14. Gauge 14 is positioned at the end of the first explosive. Air has lower impedance and thus would reduce the peak pressure at that location. Impedance is the product of the material density and its bulk sound speed. Hence as the pressure wave travels through the air gap, its peak pressure gradually decreases. .The average wave velocity through air is 2.3km/s. For a gap distance of 100mm, the time taken for the wave to travel through the air is approximately $44\,\mu$s. This is consistent with the time shown in Figure 17. Although the peak pressure reduces as it is traveling through the air gap, it can be seen from Figure 17 that the incident pressure at the air gap/acceptor explosive interface was sufficient to initiate detonation. Hence, to avoid sympathetic detonation there is a need to increase the air gap length.
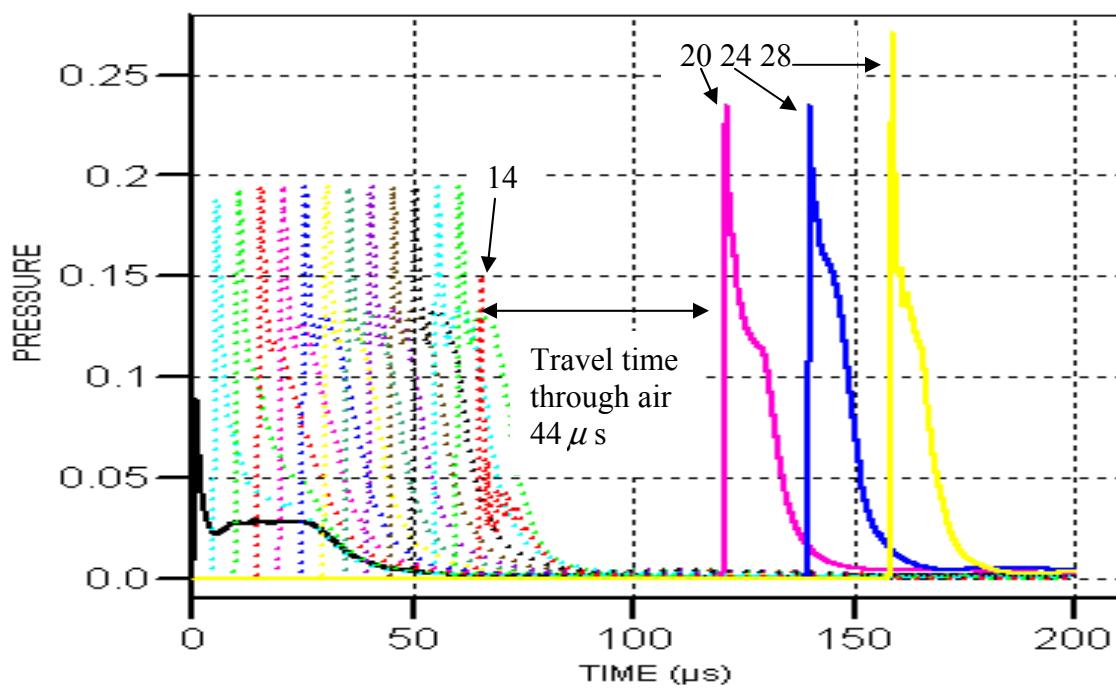
Figure 17.   Head-On 100mm Air Gap Simualtion

b. *300mm Air Gap*

In this simulation the air gap was increased to 300mm and Figure 18 shows the results of the simulation.
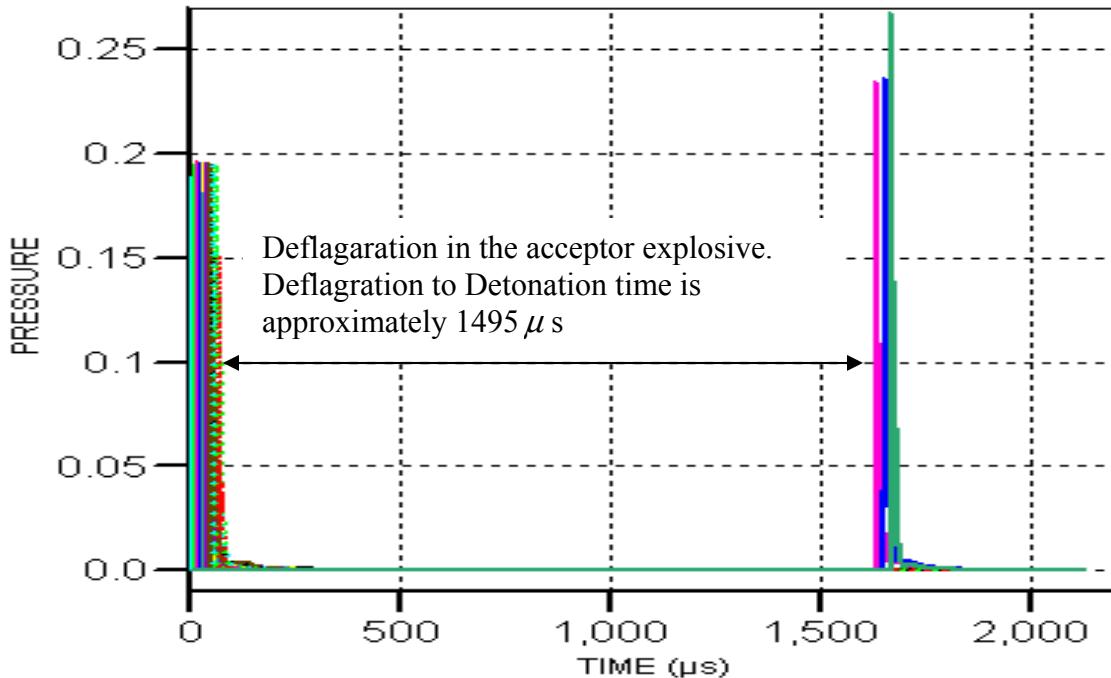
Figure 18.   Head-On 300mm Air Gap Simulation

It can be seen from Figure 18 that the detonation in the acceptor explosive only occurs at approximately 1700 μs. The time taken for the detonation wave to travel through the donor explosive is approximately 75 μs. The time take for the pressure wave (traveling at 2.3km/s) to travel through a 300mm air gap is approximately 130 μs. Therefore the incident pulse would have reached the air gap/acceptor explosive interface at approximately 205 μs. Figure 18 shows that detonation in the acceptor explosive only occurred after 1700 μs suggesting that there was burning in the acceptor explosive for a good proportion of the time.   Although the incident pressure wave was weaker it was strong enough to initiate detonation in the acceptor explosive.

c. *800mm Air Gap*

At an air gap of 800mm detonation only occurred in the donor explosive as the pressure wave after traveling through the 800mm air gap was too weak to initiate detonation in the acceptor explosive. Table 8 summarizes the estimated times for the arrival of pressure wave at the air gap/acceptor explosive interface and time at which detonation occurred in the acceptor explosive for air gaps 100mm to 800mm.

Table 8.   Head On 100mm-800mm Air Gap Estimated Pressure Wave Arrival Time and Acceptor Explosive Detonation Time

Air Gap Distance (mm)	Time of arrival at Gap/Acceptor explosive interface (μ s)	Time required to reach full detonation (μ s)
100	119	120
200	162	160
300	205	1700
400	249	2100
600	336	2300
800	423	No Detonation

d.   ***Discussion Head-On Orientation***
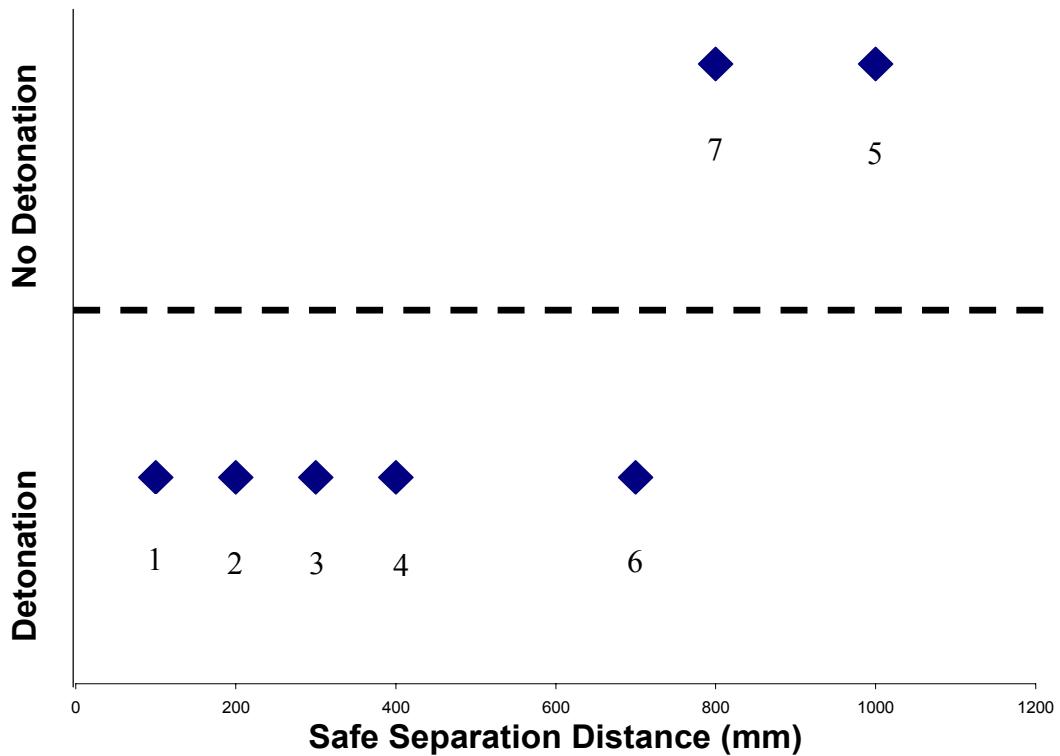
Figure 19.   Safe Separation Distance Head-On Orientation

Based on the above results it can be concluded that two 520mm explosive blocks placed in an head-on orientation would require a minimum safe separation distance of 800mm or 1.5 times the length of the detonated explosive. The numbers on Figure 19 indicate the sequence of the simulation exercise which is similar to the process used in experimental work. After sequence 4 (400mm), the next simulation was conducted at a safe separation distance of 1000mm. Once it was realized that the minimum safe separation distance was between 400mm and 1000mm, the deduction process for determining at a safe separation distance of 800mm is easily arrived.

At a 700mm air gap the acceptor charge detonated and at 800mm air gap the acceptor charge did not detonate. Observing the 700mm pressure trace reveals that the incident peak pressure and duration prior to detonation is low (1GPa peak pressure). However the 800mm air gap did not show any pressure ripples. The pressure ripples observed in the 700mm air gap case may suggest burning within the acceptor explosive

44

which subsequently led to a detonation. This seems to suggest a case of deflagration reaction growing into a full steady-state detonation. An analysis on the effects of deflagration to sympathetic detonation need to be studied in future analysis.

In the head-on simulation the direction of the traveling pressure wave and the central axis of the acceptor explosive are in line. In the side on simulations, the axes are in parallel and the next set of simulations would reveal the impact of having the explosives place in this orientation.

2. Side-On Simulations

The set up for side on simulation is shown in Figure 20. In this set up the acceptor explosive is placed parallel to the donor explosive (the explosive with the detonator). Similar to the head on test, the gauge in the donor explosive are along its central axis at 40mm intervals. On the acceptor explosive, four gauges placed 10mm vertically from each other and at 100mm intervals.[6] This orientation allows us to confirm that the pressure wave is expanding radially as the results show a slight difference in time between two vertically placed adjacent gauges.

---

[6] Gauge locations are presented in Appendix D.
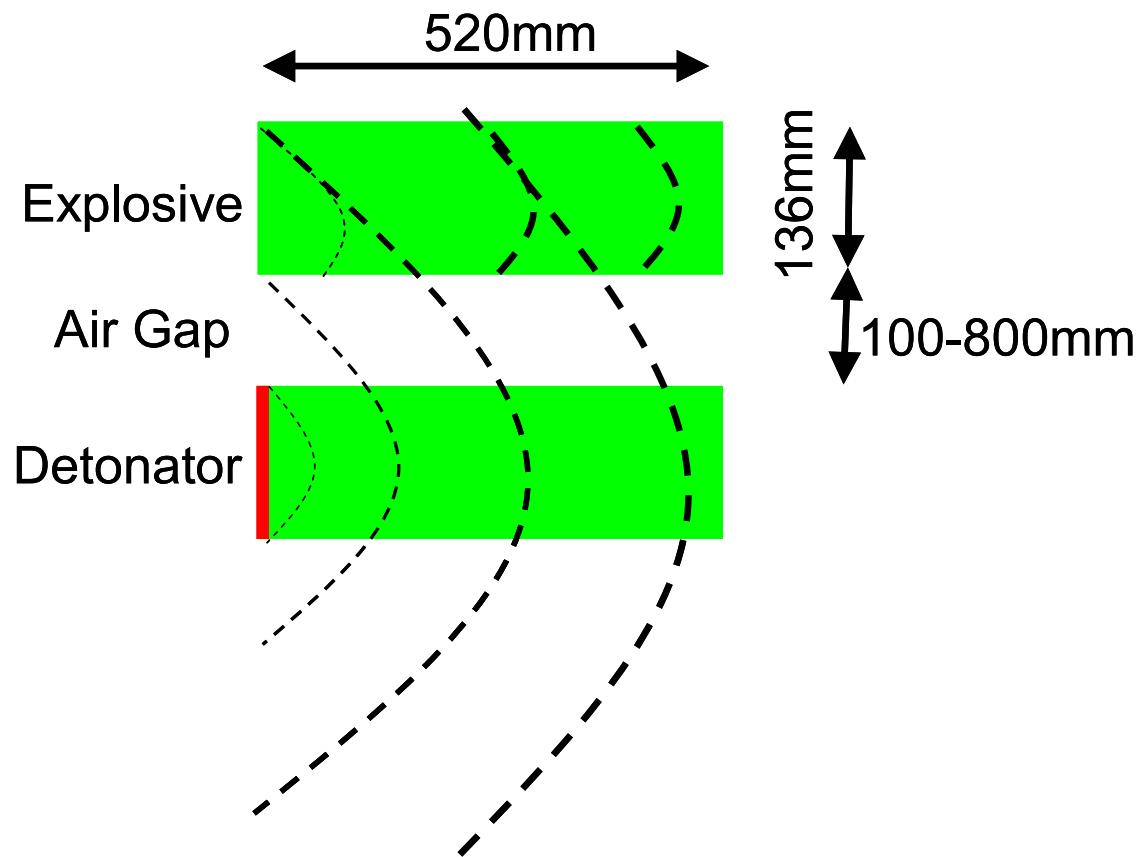
Figure 20.   Side-On Simulation Set Up

a   *100mm Air Gap*

In the first simulation, the air gap between the two explosive blocks was at 100mm. Figure 21 shows the peak pressure results for this simulation. For simplicity only gauges 20, 24, 28, 32, and 36 (in the acceptor explosive) are shown. The pressure readings on the y-axis are in 100GPa.
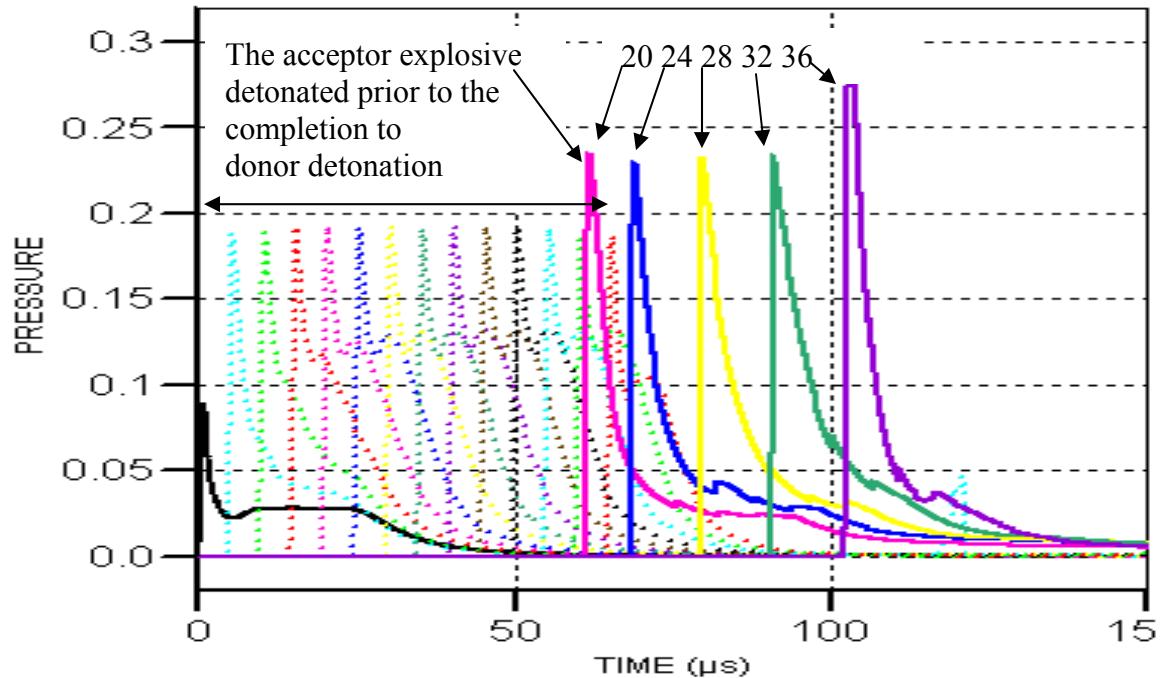
Figure 21.   Side-On 100mm Air Gap

It can be seen that the acceptor explosive detonates 60μs after the donor explosive is detonated. The time taken for the pressure wave to travel through 100mm air gap is 44μ s. On reaching the acceptor explosive, Figure 21 suggest that the run-up to detonation in the acceptor explosive is approximately 16μ s, thus giving steady state detonation at 60μ s. The incident pressure wave is strong as the acceptor explosive detonates almost instantly.

Summary of the 100-600mm Air Gap Side-On Results

Following the results of the 100mm air-gap side-on orientation, the air gaps was increased to 600mm. At this distance no sympathetic detonation was observed. The subsequent gap size at 300mm and 500mm caused sympathetic detonation. A summary of results are presented in Figure 22 and Table 9.
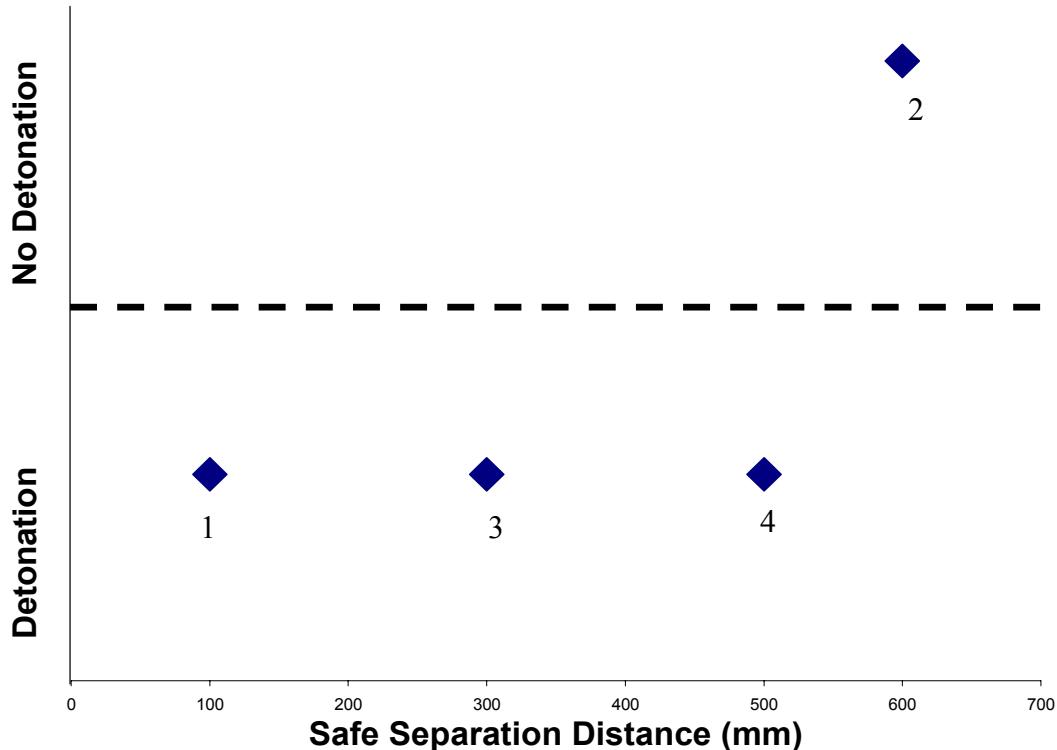
Figure 22.   Safe Separation Distance Side On Orientation

Table 9.   Side On 100mm-600mm Air Gap Estimated Pressure Wave Arrival Time and Acceptor Explosive Detonation Time

Air Gap Distance (mm)	Time of arrival at Gap/Acceptor explosive interface (μ s)	Time required to reach full detonation (μ s)
100	44	60
300	130	2400
500	217	2500
600	261	No Detonation

Based on the above results it can be concluded that in the side-on orientation the safe separation distance is 600mm. The radially expanding pressure wave imparts a lower impulse onto the acceptor explosive thus resulting to a lower safe separation distance.

3. Insights from Large Scale Simulations

In the large scale simulation the explosive mass was kept constant and only the orientation was altered. The simulation demonstrated that by having the acceptor explosive in the side-on orientation, it reduced the safe separation distance by 25% when compared to the head-on orientation.

Hence, it is reasonable to conclude that a radially expanding pressure wave reduces in strength faster than an axially traveling pressure wave. As previously discussed the safe separation distance $R_{Head-On} \propto$ (Donor Mass) $^{1/3}$ for the head-on orientation scenario. However, the large scale simulation results do suggest that in an side-on orientation $R_{Side-On} = 0.75 R_{Head-On.}$ Hence, knowledge of the traveling pressure wave is necessary as it allows for safer and more optimum use of storage space.

THIS PAGE INTENTIONALLY LEFT BLANK

VI. CONCLUSION

The simple model for ideal detonation was introduced to understand the physics behind a detonation. Subsequently two techniques, one based on chemical structures and the other on thermochemistry, for determining the detonation velocity and pressure for explosives were presented. The Chapman-Jouguet state is where the Raleigh line, a line joining the initial state of the explosive to its final compressed but unreacted state, is at tangent to the product Hugoniot. It is at the Chapman-Jouguet state that the reaction zone, rarefaction front and shock front are all traveling at the same velocity.

The cell size of 4mm and an interaction gap size of 0.12mm best describe the detonation characteristic of the Composition B explosive when using the AUTODYN codes, Lagrange-Lagrange interaction with Lee Tarver ignition and growth model. Simulations results using these sizing showed good agreement with both experimental and least square fits for Composition B. Our validation trials conducted on 15mm, 20mm and 32mm Plexiglas gap lengths generated run distances and sympathetic detonation characteristics that agreed with Kubota's experimental results. They were also compared with the least square fits for Composition B and both results show good correlation.

A methodology was established to understand the likelihood of sympathetic detonation for existing and future explosives. The sympathetic detonation of high energetic materials is affected by the peak pressure and duration of the incident shock pulse. The incident impulse is directly related to the donor mass as an increased mass sustains its peak pressure through the air gap and increase its duration. Increasing the separation distance between two adjacent explosive reduces the incident impulse. Also demonstrated from the large scale simulations is the need to consider explosive spatial orientation. As shown, the side-on orientation reduces the safe separation distance by 25% when compared to the head-on orientation. The methodology developed allows for proper determination of safe separation distance from shock-blast effects.

THIS PAGE INTENTIONALLY LEFT BLANK

VII. RECOMMENDATION

It has been established that an increase in the donor mass would lead to an increase in duration of the incident pressure wave. Analysis can be made to investigate the relationship between the duration of the incident pressure wave and donor size.

An uncertainty in the simulation exercise is the detonation characteristics of the detonator. This uncertainty may be removed by the insertion of a booster explosive between the detonator and donor. With the detonation pressure and velocity of the booster explosive known, the incident pulse into the donor explosive is established. The relationship of the incident pulse on the donor peak pressure can also be studied

A primary propagation mechanism for sympathetic detonation is fragment penetration from the donor weapon. A natural progression to this thesis would then be the inclusion of the effects of fragmentation in the methodology. This analysis is currently being pursued at NPS.

To improve the realism of the simulations, all vulnerable elements of the target ammunition in terms of its safe and arm mechanism, booster and main charge explosives and all protective elements for shock mitigation should be modeled. Early studies indicate porous materials as effective to prevent sympathetic detonation for closely packed systems as they are good shock energy absorbers. Porous materials such as pumice have demonstrated to have good properties for shock mitigation. [10]

Lastly all energetic materials are sensitive to heat as they may experience degradation or decomposition which may lead to an ignition. A study on the effects of explosive temperature on to detonation could be investigated. The slow cook-off test is a means to investigate the sensitivity of the explosive to heating.

THIS PAGE INTENTIONALLY LEFT BLANK

APPENDIX A   MODEL VALIDATION WITH COMPOSITION B
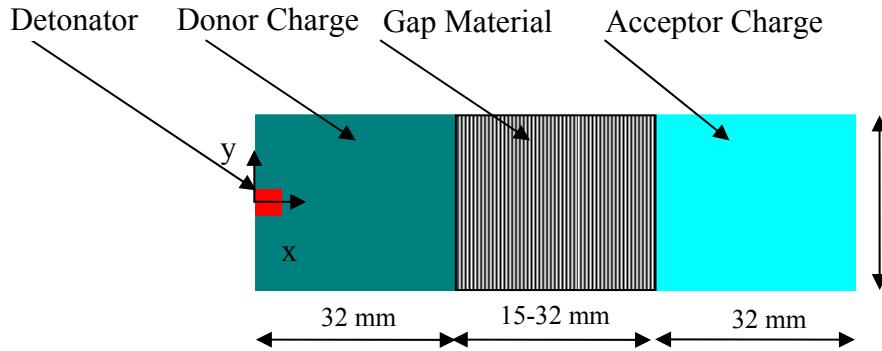
Figure A-1 Model Validation Set for Plexigals Gaps 15-32mm

In the model validation for Composition B, gauges were placed along the central longitudinal axis (defined as y = 0).

In the need to ascertain run distance for 15 and 20mm Plexiglas gap, more gauges at 1mm intervals were place in the leading edge of the acceptor charge. At all other locations the materials were spaced at 4mm intervals.

The gauge locations are shown in Table A-1. Note, the y-axis = 0 for all gauges (centrally placed).

Table A-1 Gauge Location for Model Validation Trials

Gauge No	x-axis location for gauges		
	15mm Gap	20mm Gap	32mm Gap
1	0.00	0.00	0.00
2	4.00	4.00	4.00
3	8.00	8.00	8.00
4	12.00	12.00	12.00
5	16.00	16.00	16.00
6	20.00	20.00	20.00
7	24.00	24.00	24.00
8	28.00	28.00	28.00
9	33.20	33.20	33.20
10	37.20	37.20	37.20
11	41.20	41.20	41.20
12	45.20	45.20	45.20
13	46.20	49.20	49.20
14	47.20	50.20	53.20
15	48.20	51.20	57.20
16	50.00	52.20	61.20
17	51.00	53.20	62.20
18	52.00	55.40	63.20
19	53.00	56.40	64.20
20	54.00	57.40	65.20
21	55.00	58.40	67.40
22	56.00	59.40	68.40
23	57.00	60.40	69.40
24	58.00	61.40	70.40
25	59.00	62.40	71.40
26	60.00	63.40	72.40
27	61.00	64.40	73.40
28	62.00	65.40	74.40
29	63.00	66.40	75.40
30	64.00	67.40	76.40
31	65.00	68.40	77.40
32	66.00	69.40	78.40
33	67.00	70.40	79.40
34	68.00	71.40	80.40
35	69.00	72.40	81.40
36	70.00	73.40	82.40
37	71.00	74.40	83.40
38	72.00	75.40	84.40
39	73.00	76.40	85.40
40	74.00	77.40	86.40

41	75.00	78.40	87.40
42	76.00	79.40	91.40
43	77.00	80.40	95.40
44	78.00	81.40	
45	79.00	82.40	
46	80.00	83.40	
47		84.40	
48		85.40	
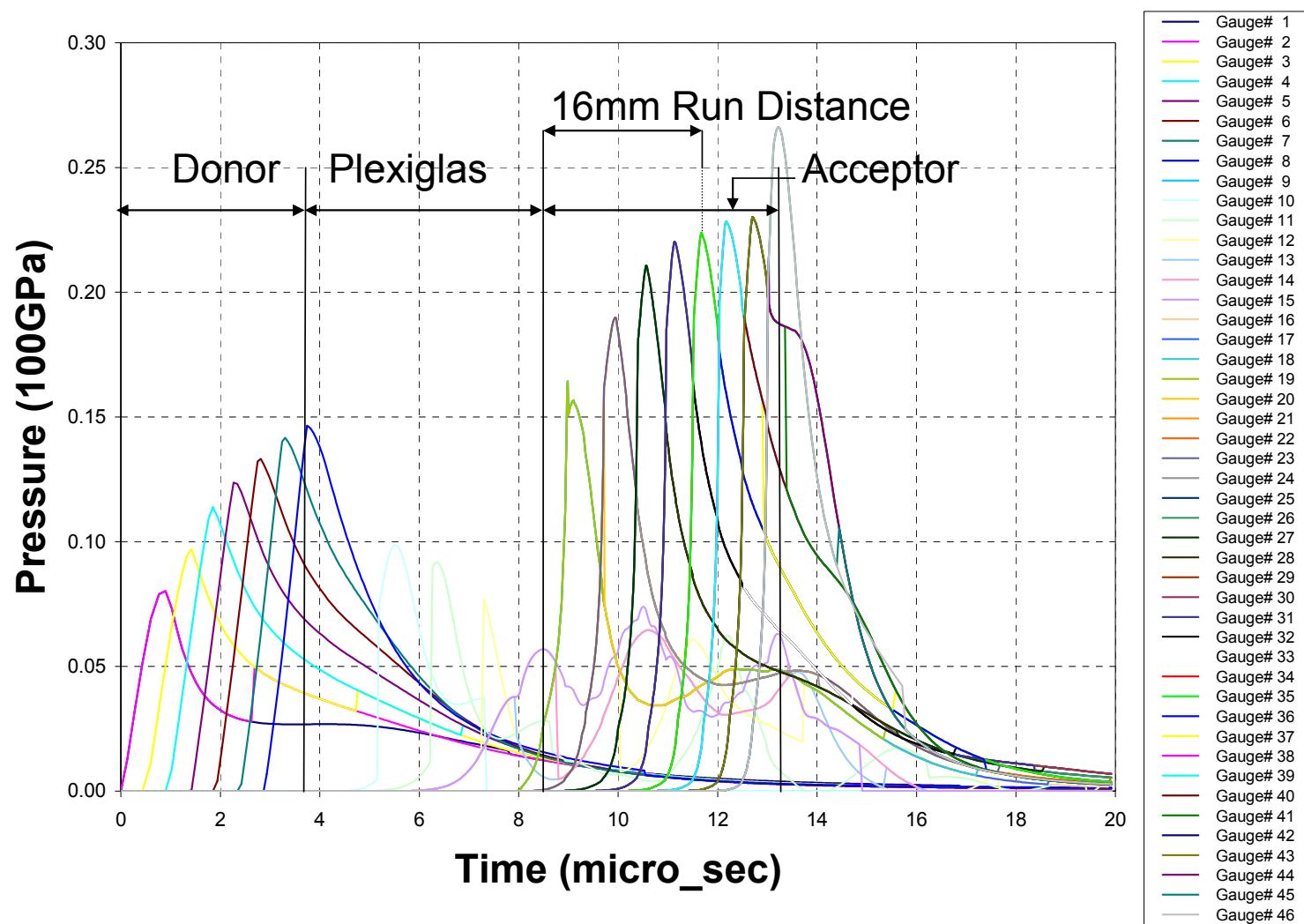
Figure A-2 15mm Plexiglas Gap Showing Sympathetic Detonation
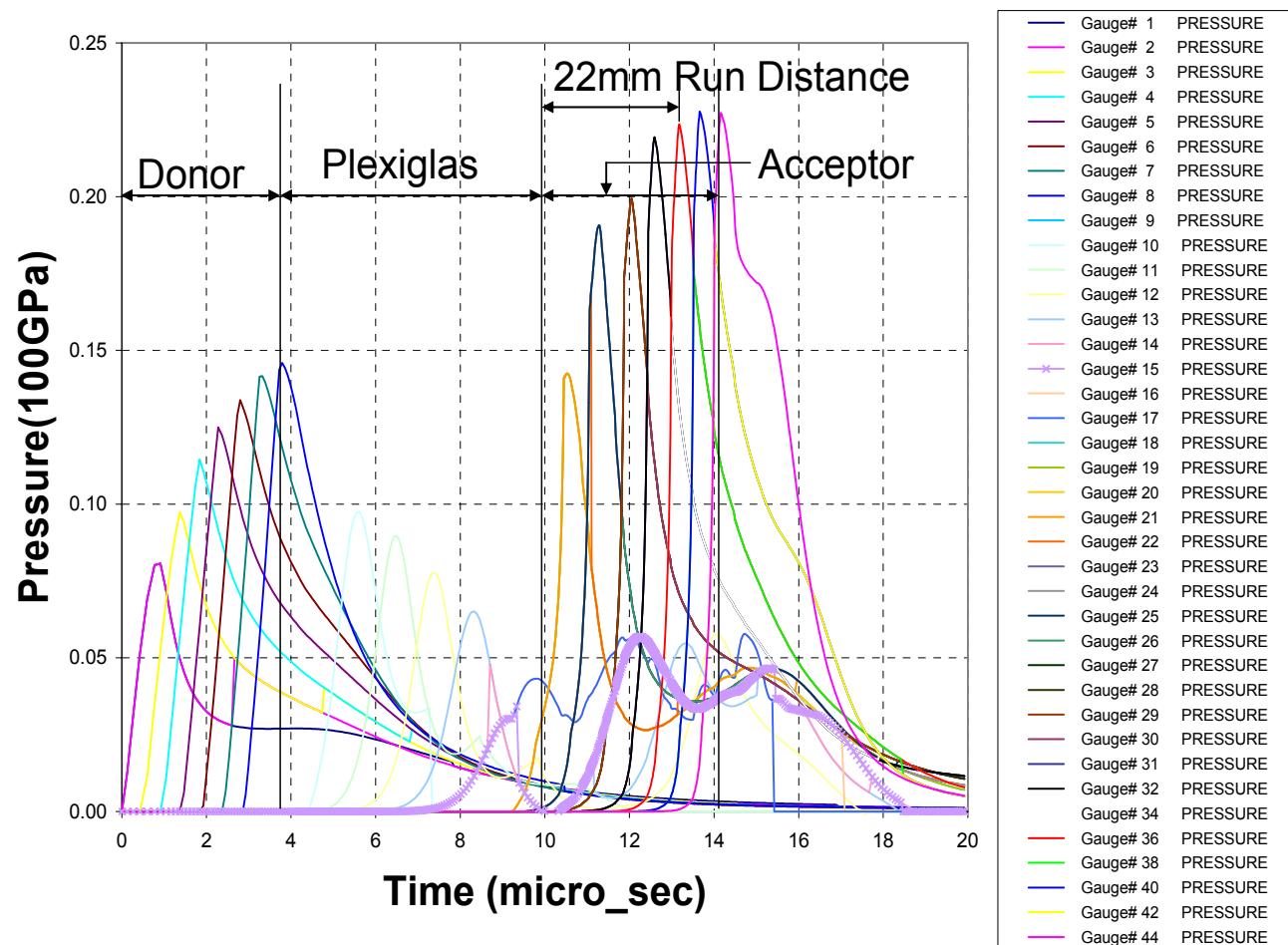
Figure A-3 20 mm Plexiglas Gap Showing Sympathetic Detonation
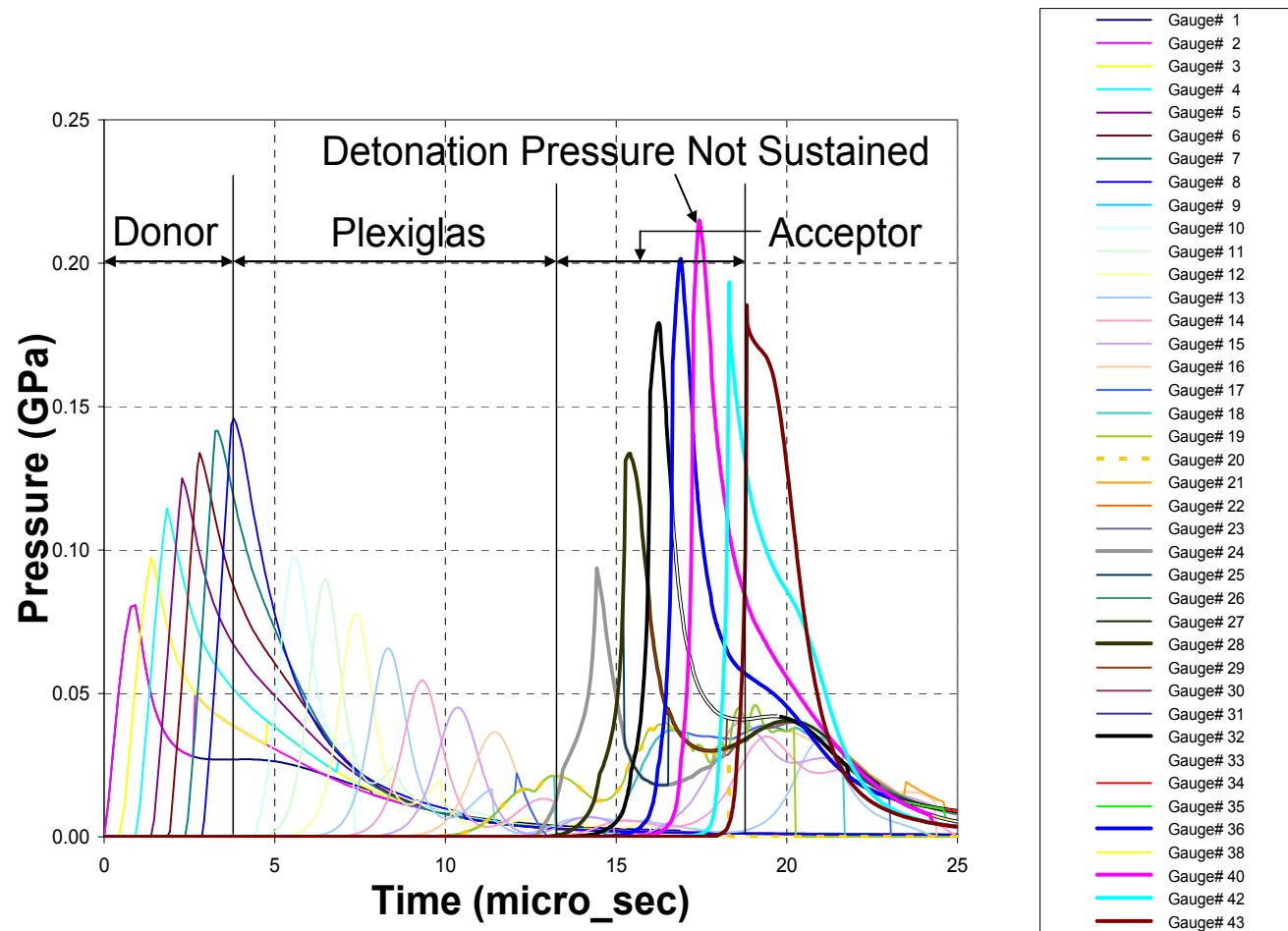
Figure A-4 32mm PLexiglass Gap Showing No Sympathetic Detonation

60

APPENDIX B   PRESSURE TIME TRACE 32-64MM DONOR CHARGES

Pressure gauges were placed at 4mm intervals along the central axis of the donor and acceptor charges
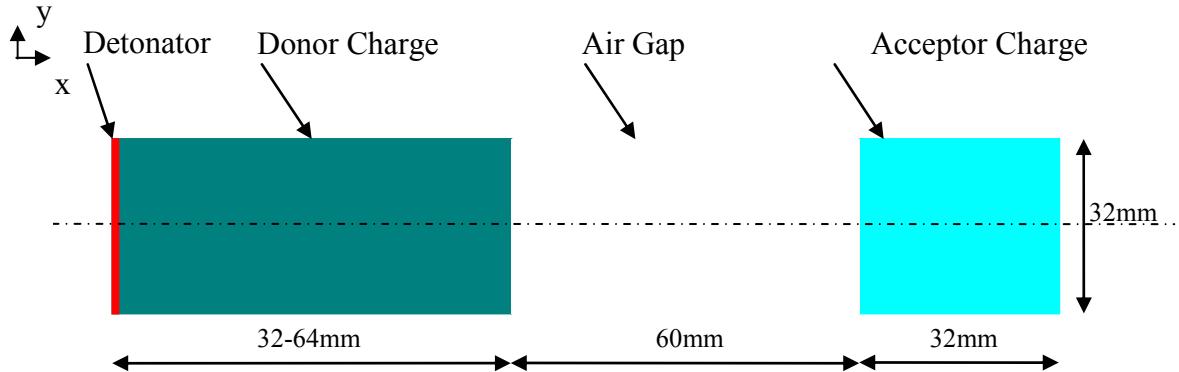
Figure B-1 Small Scale Sympathetic Detonation

The gauges are spaced at 4mm intervals in the donor and acceptor charges. They are placed along the longitudinal central axis (defined as y = 0). The x-axis location of the gauges for the different donor charges are provided in Table B-1.

Table B-1: X-axis pressure location for varying donor charge lengths.

Gauges	x- axis location for varying donor charge length				
	32mm	48mm	50mm	60mm	64mm
1	0	0	0	0	0
2	4	4	4	4	4
3	8	8	8	8	8
4	12	12	12	12	12
5	16	16	16	16	16
6	20	20	20	20	20
7	24	24	24	24	24
8	28	28	28	28	28
9	32	32	32	32	32
10	94	36	36	36	36
11	98	40	40	40	40
12	102	44	44	44	44
13	106	48	48	48	48
14	110	108	50	52	52
15	114	112	110	56	56
16	118	116	114	60	60
17	122	120	118	122	64
18	126	124	122	126	124
19		128	126	130	128
20		132	130	134	132
21		136	134	138	136
22		140	138	142	140
23			142	146	144
24				150	148
25				154	152
26					156
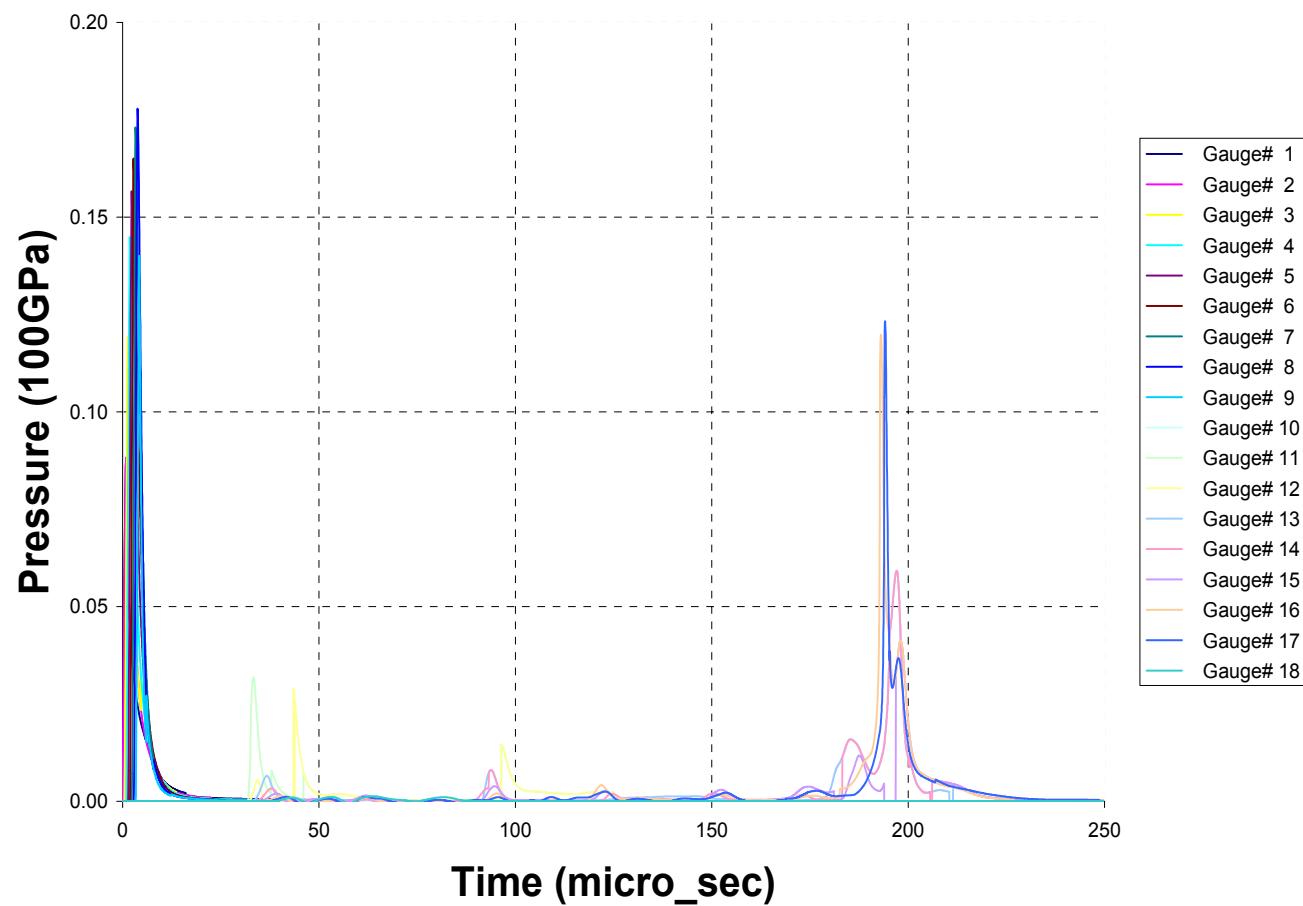
Figure B-2 Pressure Trace for 32mm Donor Length
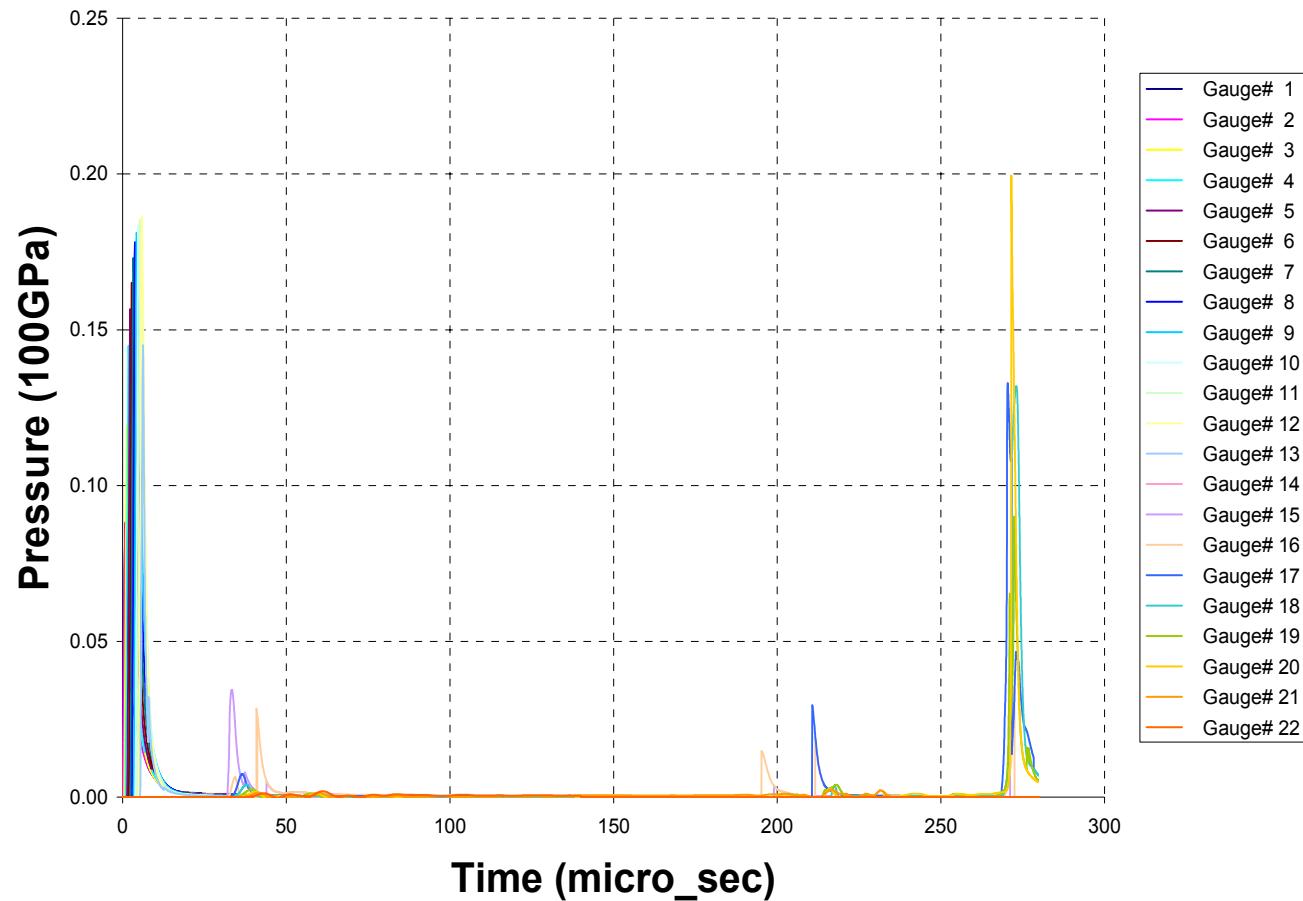
Figure B-3 Pressure Trace for 48mm Donor Charge Length
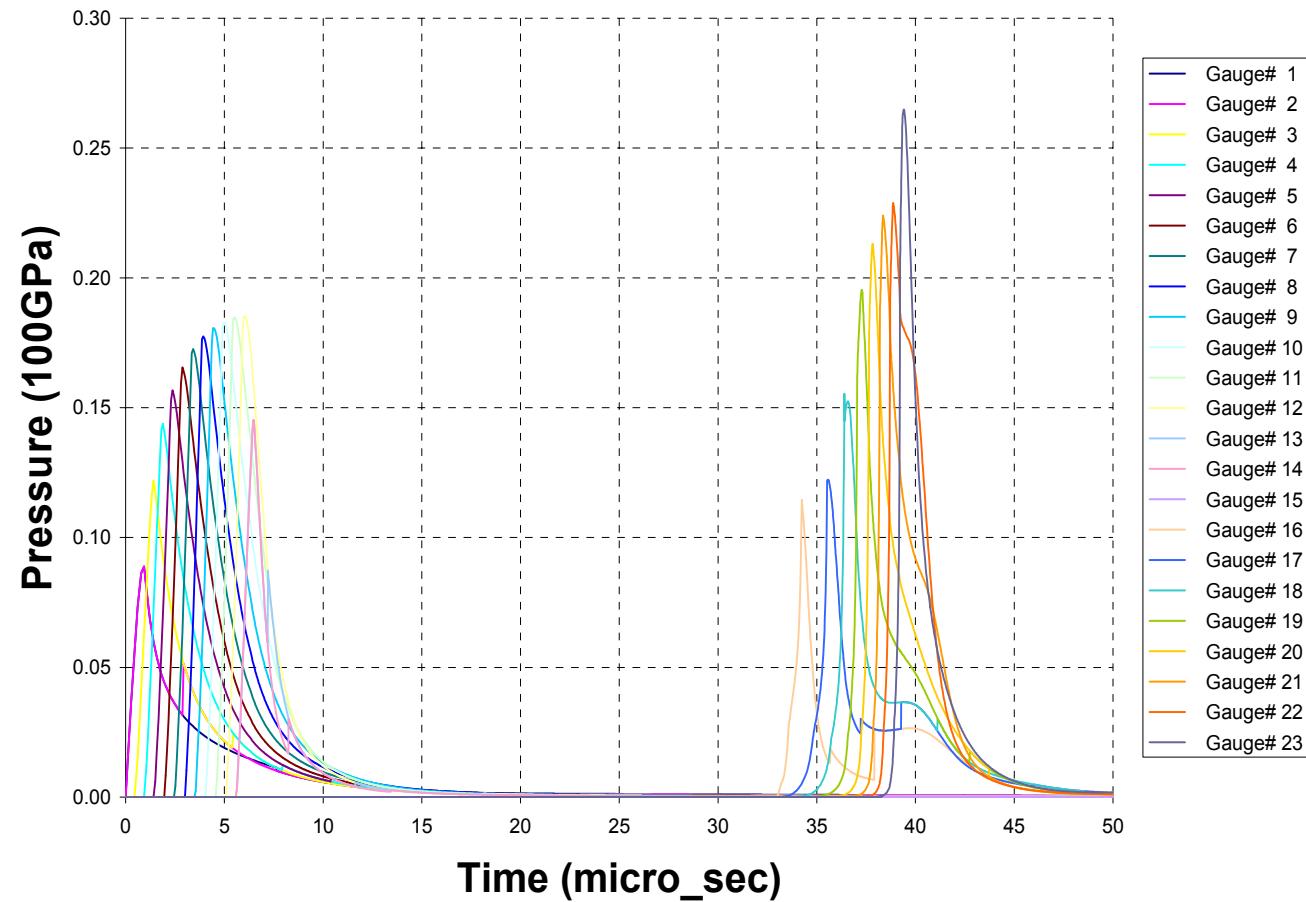
Figure B-4 Pressure Traces at 50mm Donor Charge Length
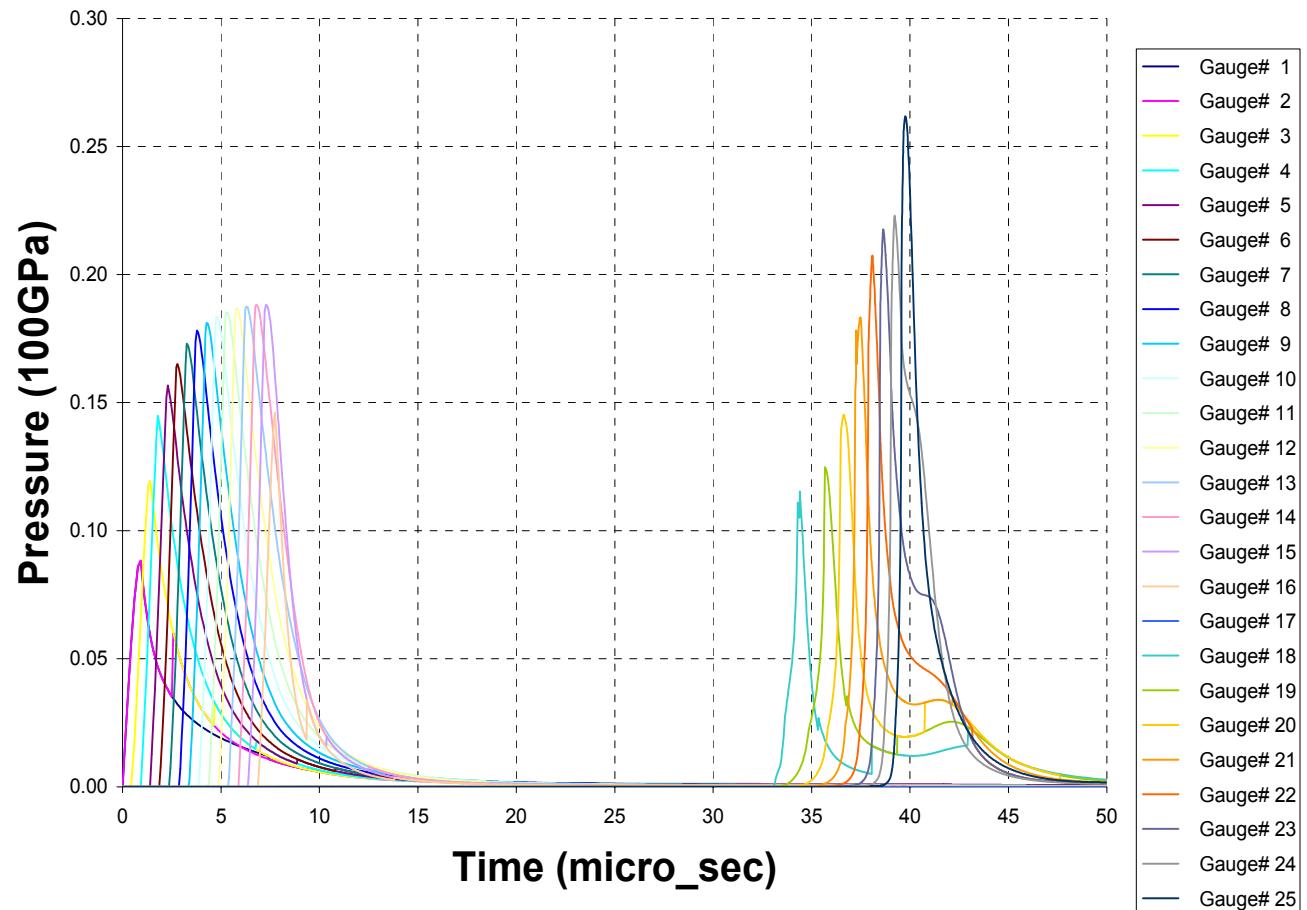
Figure B-5 Pressure Traces at 60mm Donor Charge Length
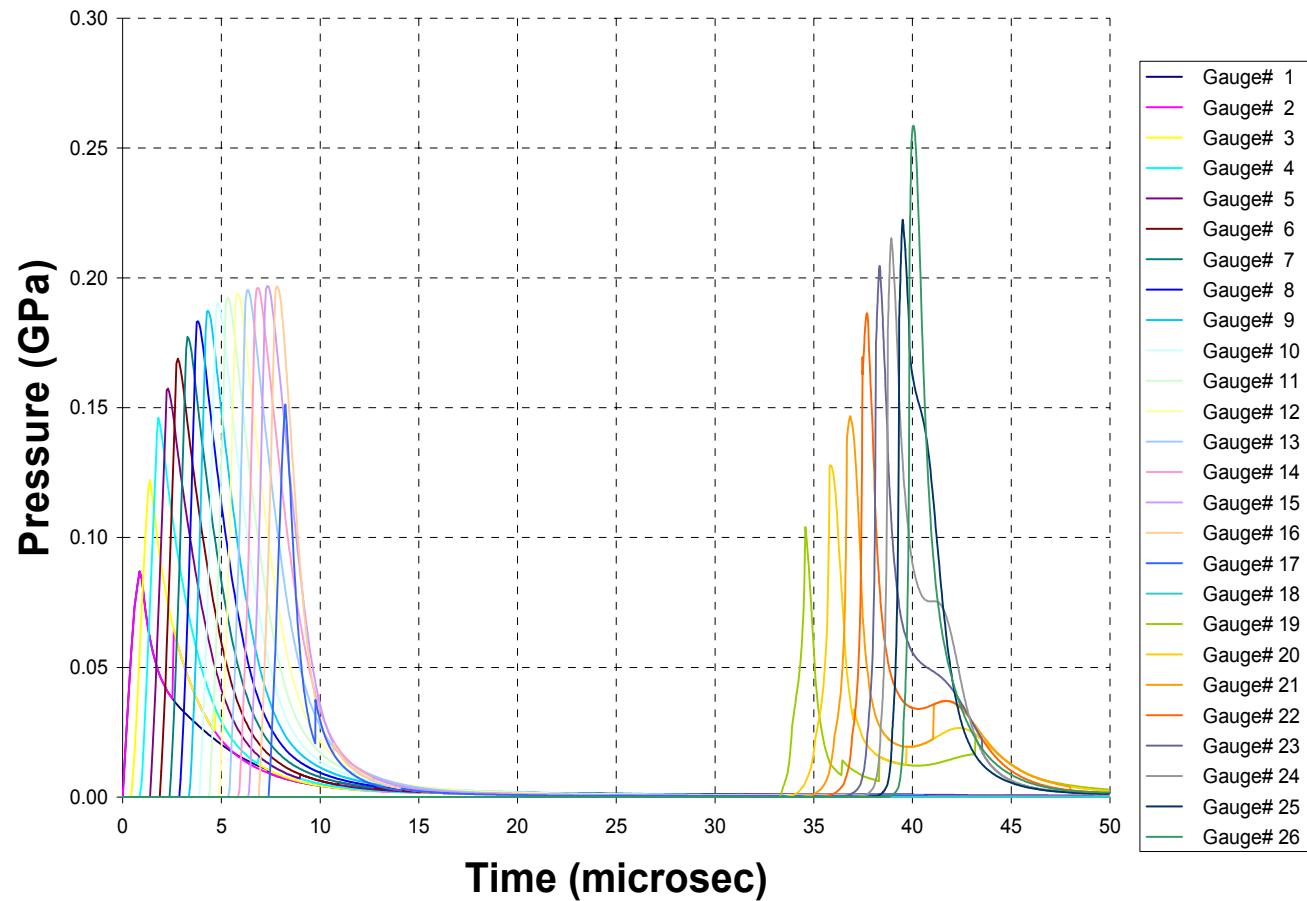
Figure B-6 Pressure Traces at 64mm Donor Charge Length

THIS PAGE INTENTIONALLY LEFT BLANK

APPENDIX C   PRESSURE TIME TRACE HEAD-ON SIMULATIONS
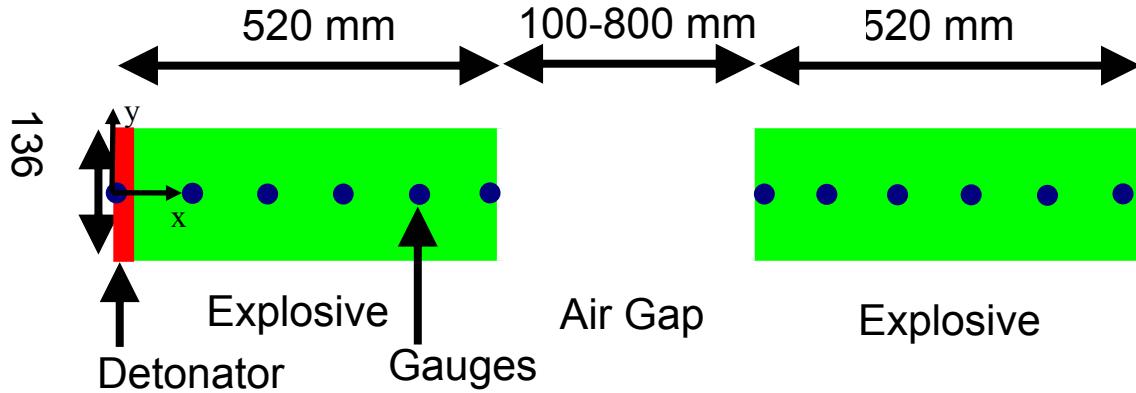
Figure C-1 Simulation Set Up For Head-On Orientation

As shown in Figure C-1 the gauges are placed central longitudinal axis (y = 0) at 40mm intervals. No gauges were place within the air gap. The gauge locations for the different air gaps are presented in Table C-1.

With reference to the pressure time plots, the pressure readings on the y-axis are at 100GPa an the x-axis is in μ s. Only the trace for gauges 20, 24 and 28 (within the acceptor explosive) is shown as the other traces show similar traces.

Table C-1 Gauge locations along the x-axis

Gauges	Air Gap Length					
	100mm	200mm	300mm	400mm	700mm	800mm
1	0	0	0	0	0	0
2	40	40	40	40	40	40
3	80	80	80	80	80	80
4	120	120	120	120	120	120
5	160	160	160	160	160	160
6	200	200	200	200	200	200
7	240	240	240	240	240	240
8	280	280	280	280	280	280
9	320	320	320	320	320	320
10	360	360	360	360	360	360
11	400	400	400	400	400	400
12	440	440	440	440	440	440
13	480	480	480	480	480	480
14	520	520	520	520	520	520
15	622	722	822	922	1220	1320
16	662	762	862	962	1260	1360
17	702	802	902	1000	1300	1400
18	742	842	942	1040	1340	1440
19	782	882	982	1080	1380	1480
20	822	922	1020	1120	1420	1520
21	862	962	1060	1160	1460	1560
22	902	1000	1100	1200	1500	1600
23	942	1040	1140	1240	1540	1640
24	982	1080	1180	1280	1580	1680
25	1020	1120	1220	1320	1620	1720
26	1060	1160	1260	1360	1660	1760
27	1100	1200	1300	1400	1700	1800
28	1140	1240	1340	1440	1740	1840
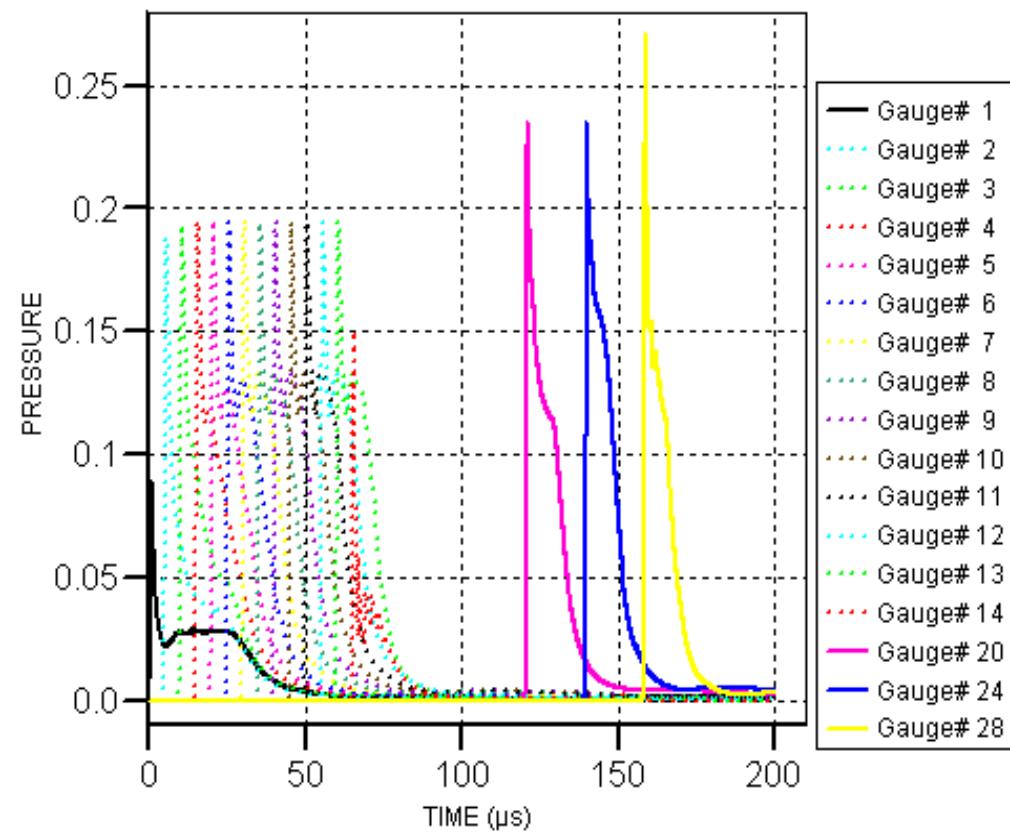
Figure C-2 100mm Air Gap Head-On
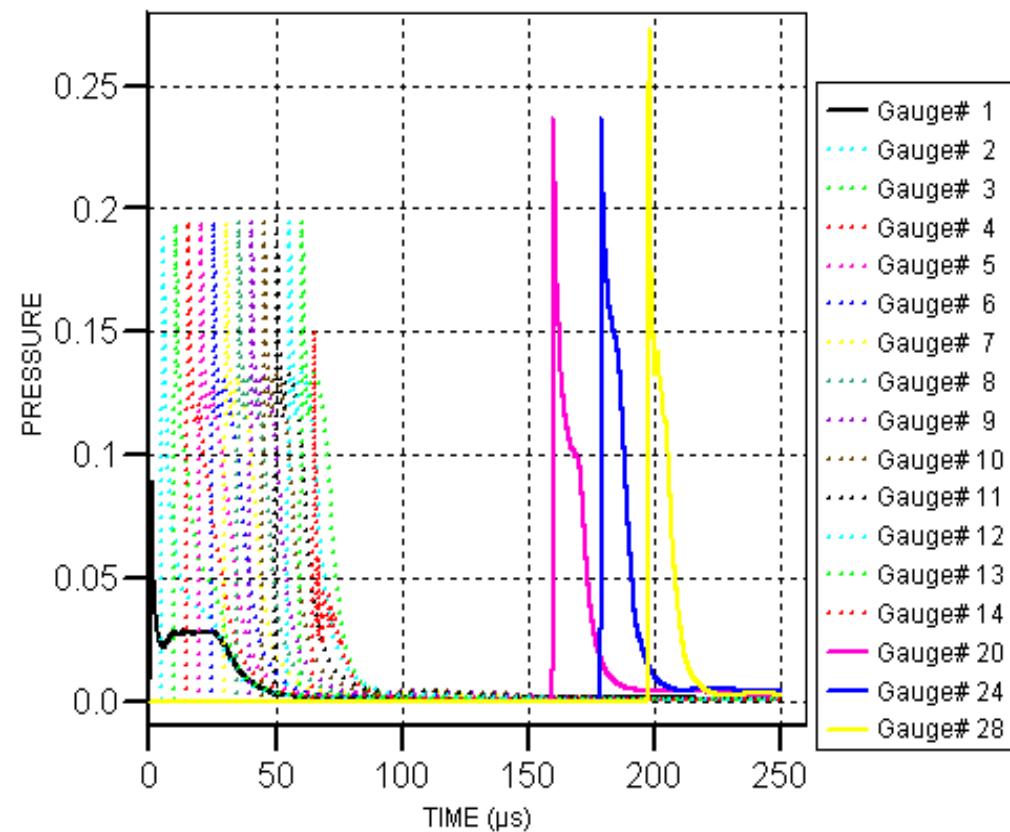
Figure C-3 200mm Air Gap Head-On
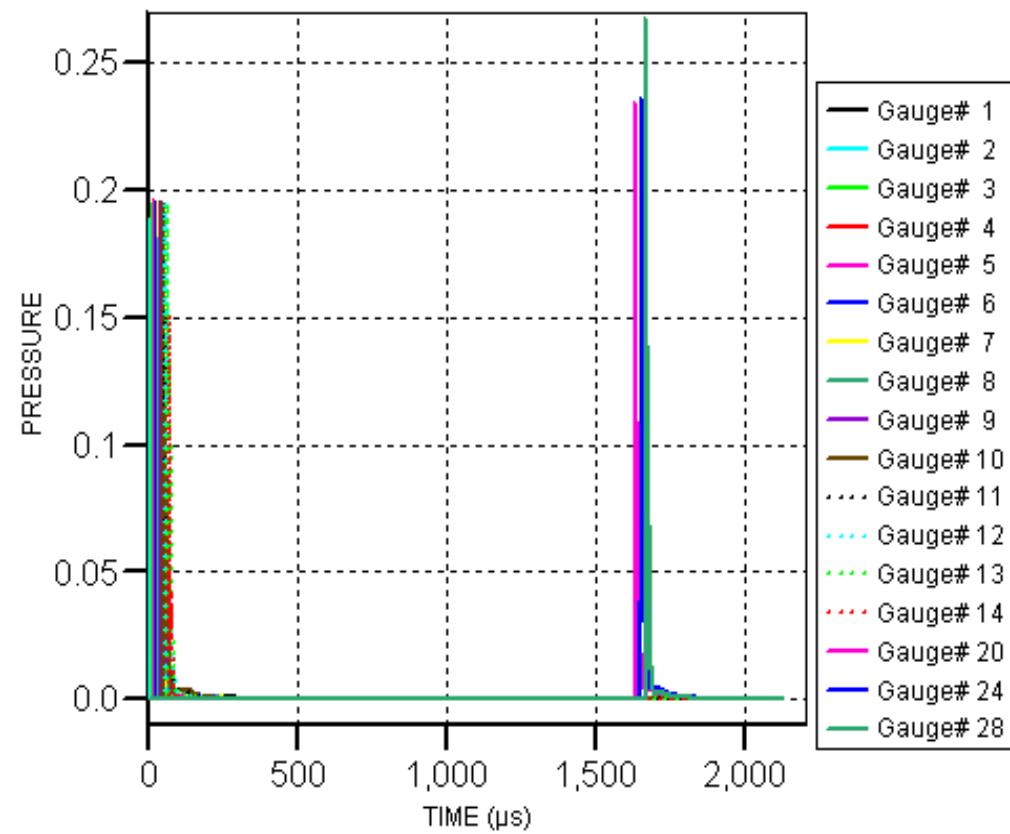
Figure C-4 300mm Air Gap Head-On
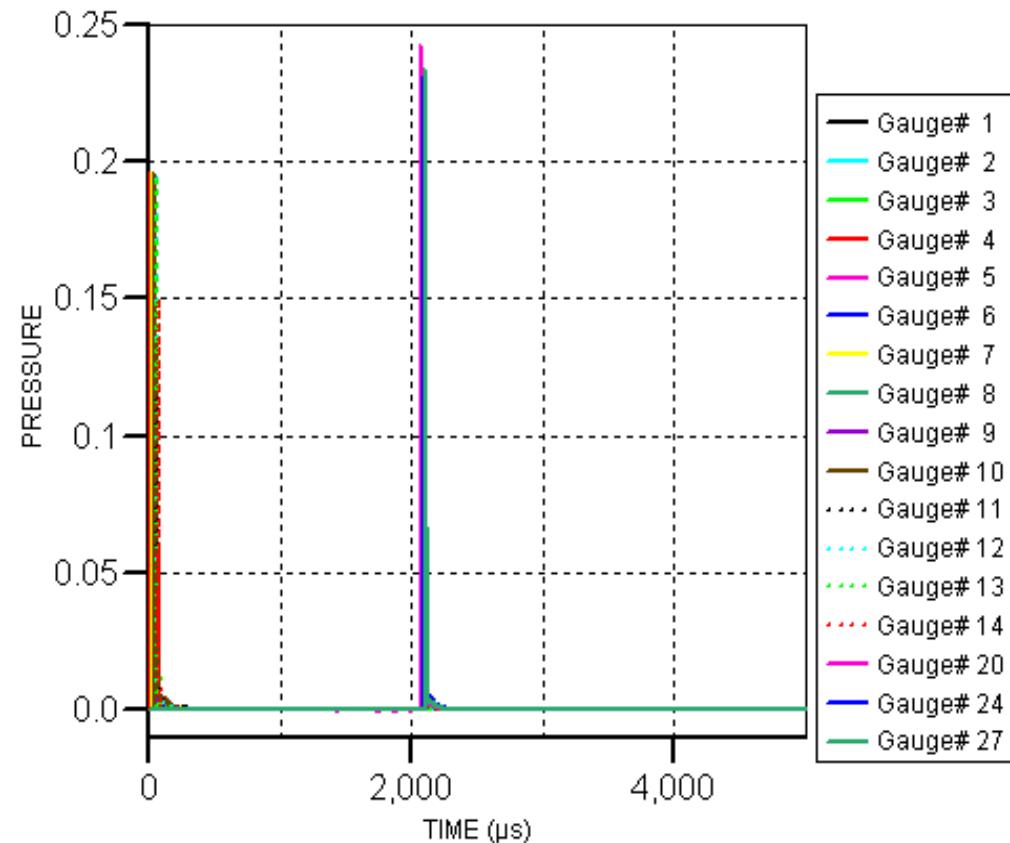
Figure C-5 400mm Air Gap Head On
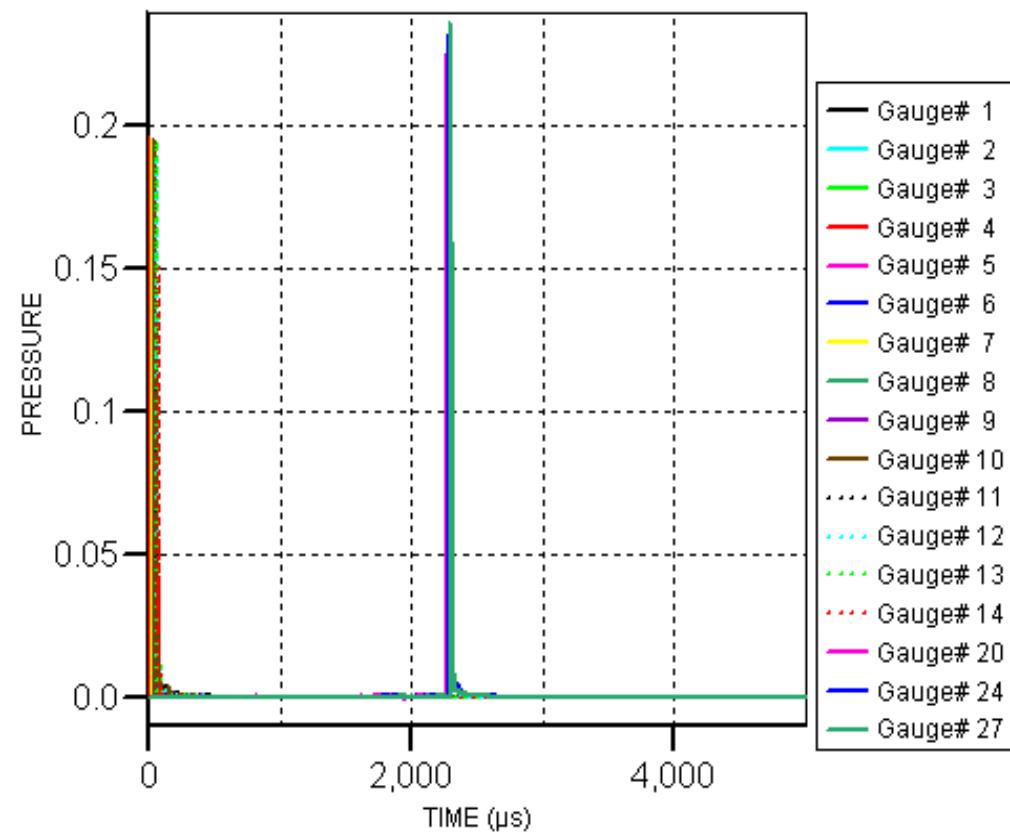
Figure C-6 700mm Air Gap Head-On
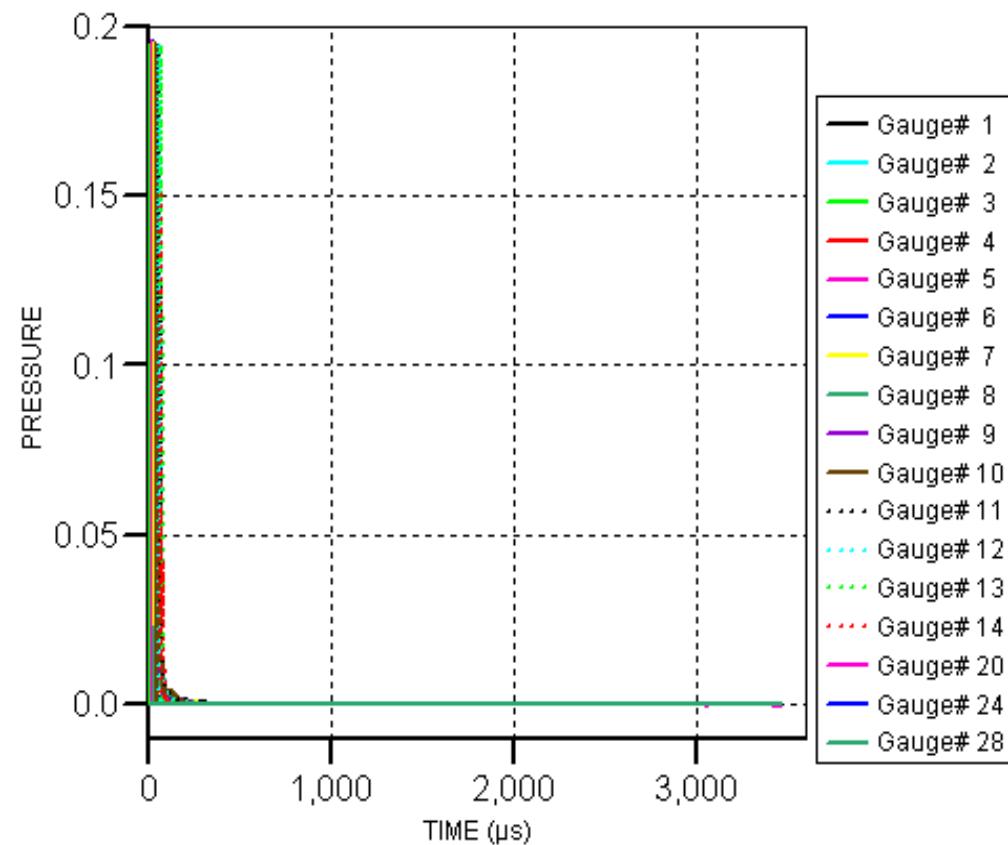
Figure C-7 800mm Air Gap Head-On

76
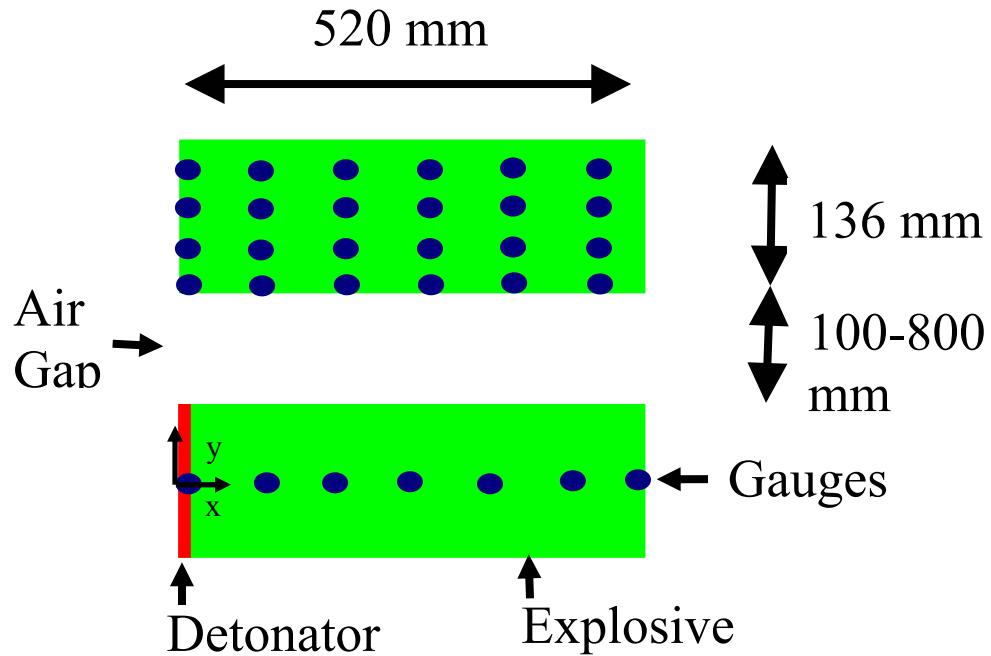
Figure D-1 Simulation Set Up For Side-On Orientation

The pressure gauges in the donor explosives are placed at 40mm intervals. The pressure gauges in the acceptor explosive are placed 100mm intervals along the longitudinal x-axis and 10mm intervals along the vertical axis. The gauge locations for the different air gaps are presented in Table D-1.

With reference to the pressure time plots, the pressure readings on the y-axis are at 100GPa an the x-axis is in μ s. Only the trace for gauges 20, 24, 28, 32 and 36 (within the acceptor explosive) is shown as the other traces show similar traces.

Table D-1 Gauge locations along the x and y axes

Gauges	100mm Air Gap		300mm Air Gap		500mm Air Gap		600mm Air Gap	
	x (mm)	y (mm)	x (mm)	y (mm)	x (mm)	y (mm)	x (mm)	y (mm)
1	0	0	0	0	0	0	0	0
2	40	0	40	0	40	0	40	0
3	80	0	80	0	80	0	80	0
4	120	0	120	0	120	0	120	0
5	160	0	160	0	160	0	160	0
6	200	0	200	0	200	0	200	0
7	240	0	240	0	240	0	240	0
8	280	0	280	0	280	0	280	0
9	320	0	320	0	320	0	320	0
10	360	0	360	0	360	0	360	0
11	400	0	400	0	400	0	400	0
12	440	0	440	0	440	0	440	0
13	480	0	480	0	480	0	480	0
14	520	0	520	0	520	0	520	0
15	0	168	0	370	0	570	0	670
16	0	208	0	410	0	610	0	710
17	0	248	0	450	0	650	0	750
18	0	288	0	490	0	690	0	790
19	100	168	100	370	100	570	100	670
20	100	208	100	410	100	610	100	710
21	100	248	100	450	100	650	100	750
22	100	288	100	490	100	690	100	790
23	200	168	200	370	200	570	200	670
24	200	208	200	410	200	610	200	710
25	200	248	200	450	200	650	200	750
26	200	288	200	490	200	690	200	790
27	300	168	300	370	300	570	300	670
28	300	208	300	410	300	610	300	710
29	300	248	300	450	300	650	300	750
30	300	288	300	490	300	690	300	790
31	400	168	400	370	400	570	400	670
32	400	208	400	410	400	610	400	710
33	400	248	400	450	400	650	400	750
34	400	288	400	490	400	690	400	790
35	500	168	500	370	500	570	500	670
36	500	208	500	410	500	610	500	710
37	500	248	500	450	500	650	500	750
38	500	288	500	490	500	690	500	790
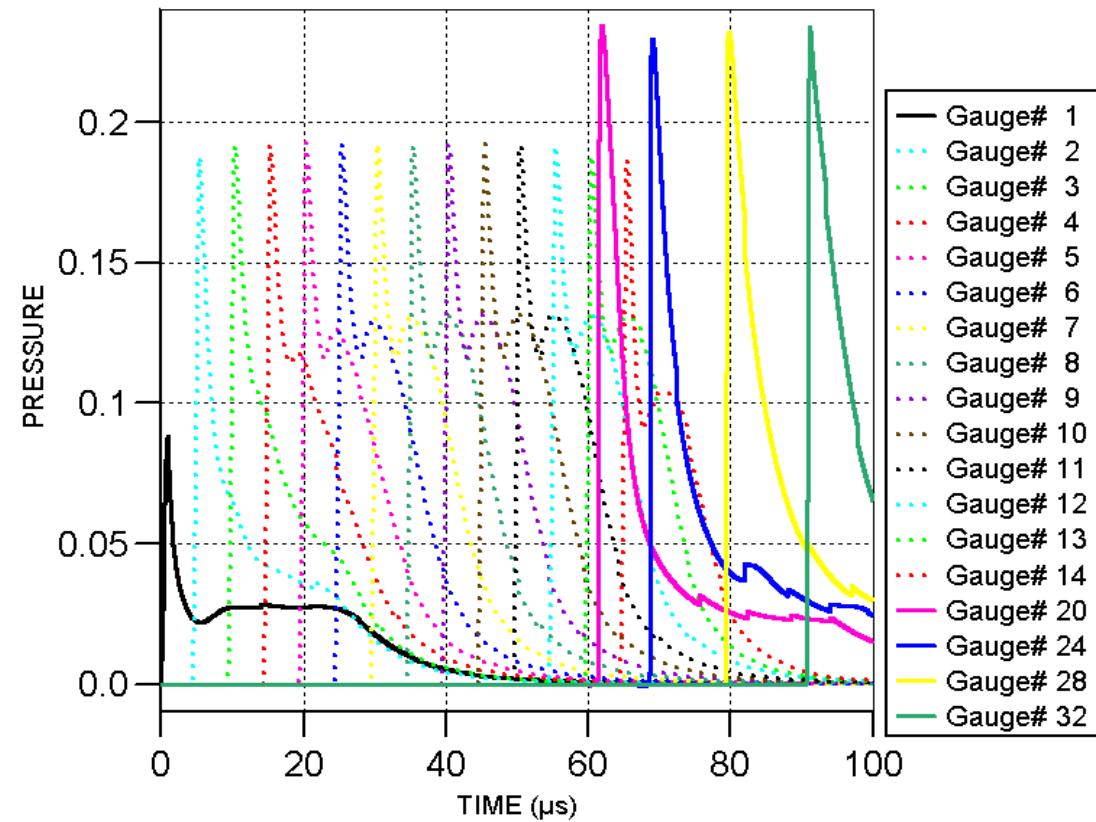
Figure D-2 100mm Air Gap Side-On
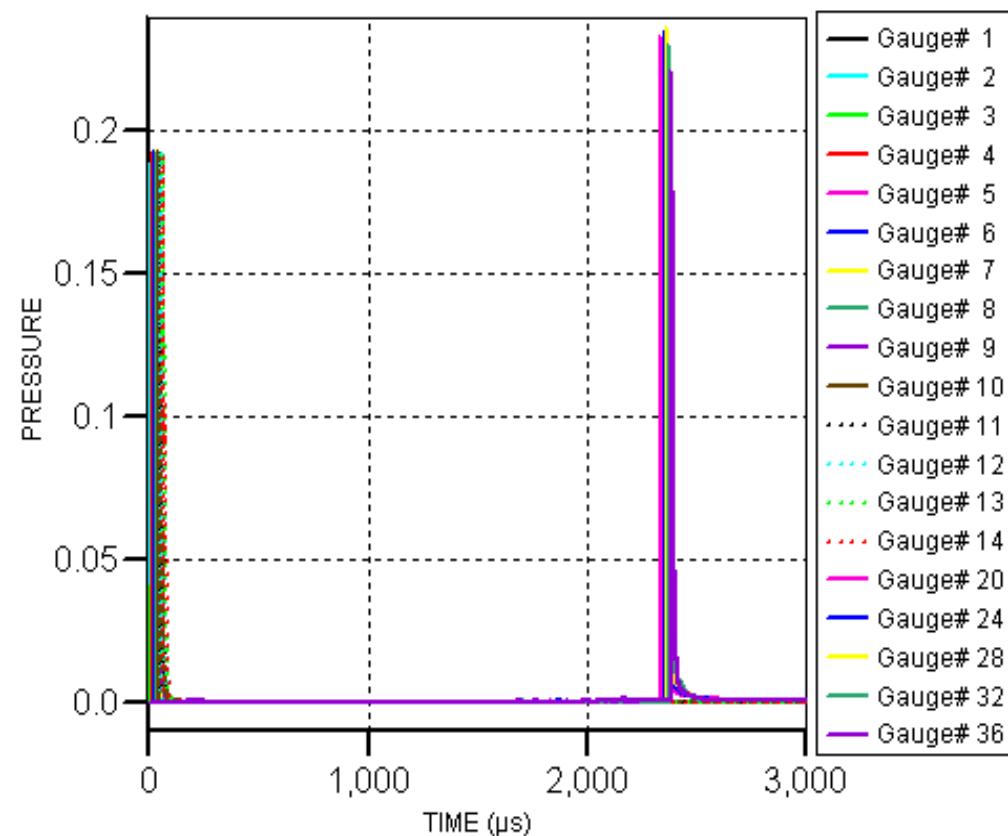
Figure D-3 300mm Air-Gap Side-On
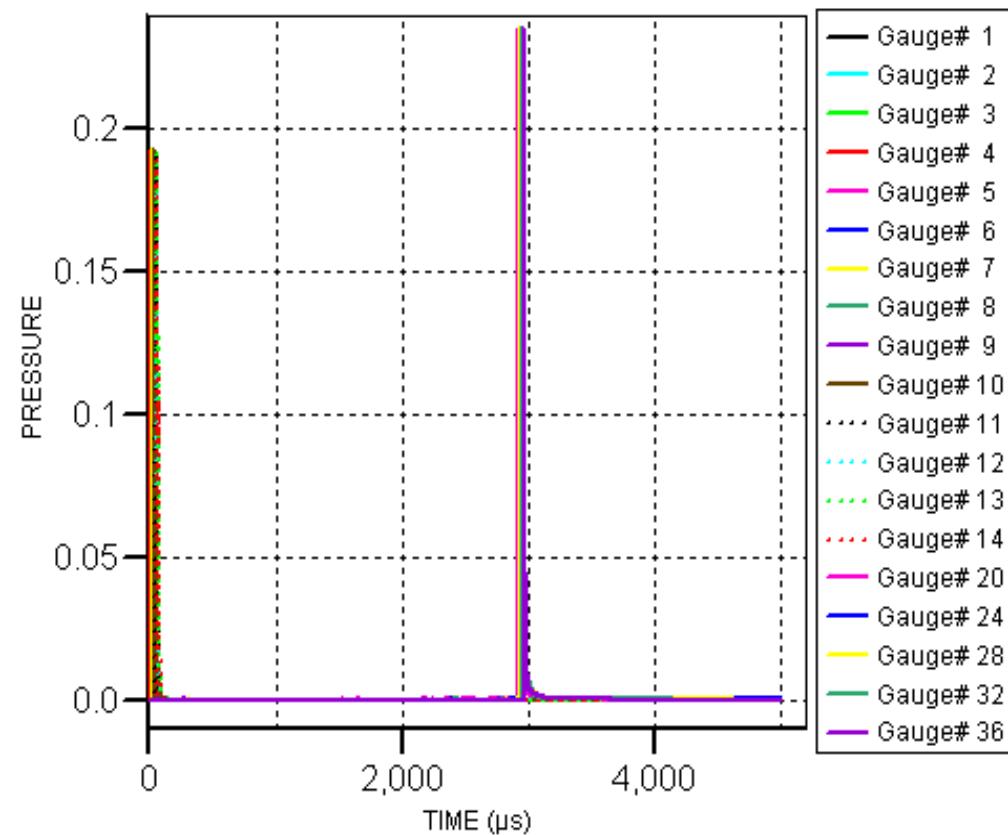
Figure D-4 500mm Air Gap Side-On
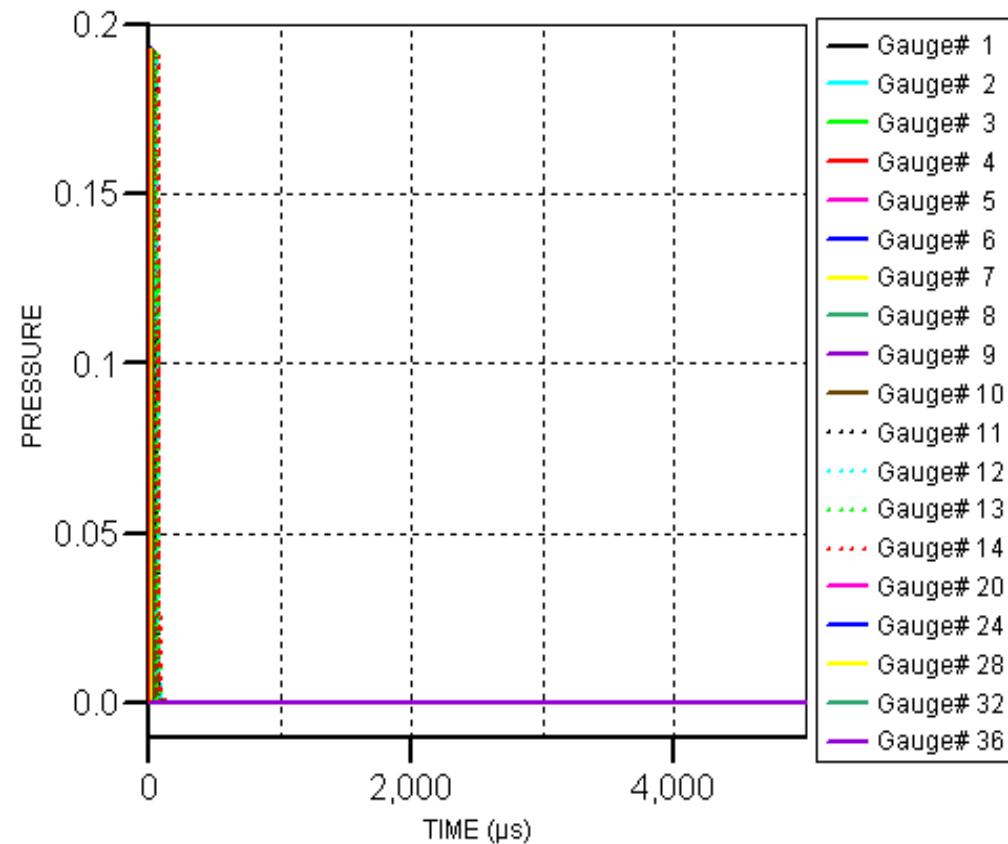
Figure D-5 600mm Air Gap Side-On

APPENDIX E   AUTODYN SIMULATION SET UP DETAIL

The following detail is an example of the procedures needed for modeling a head-on orientation (shown below) for two adjacent Composition B explosive with a 100mm safe separation distance.
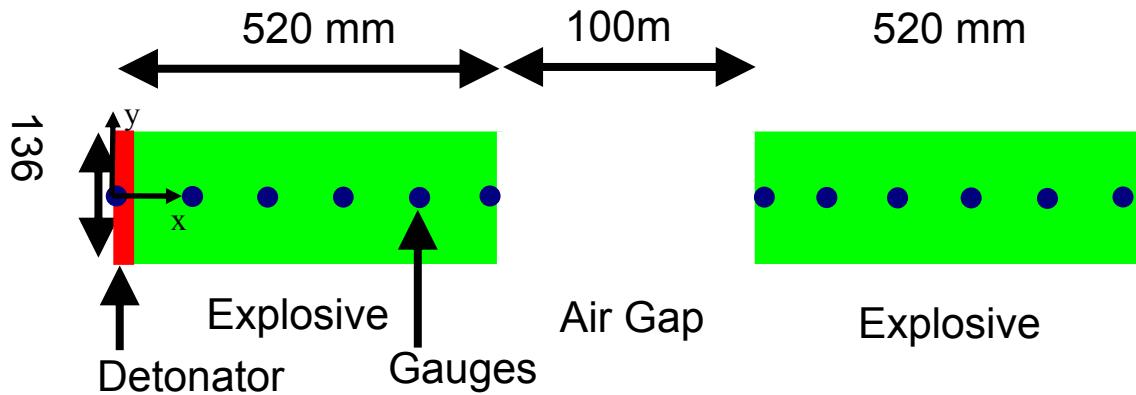
Figure E-1 Head-On Simulation Model for 100mm Air Gap

1.   Create a folder called Example in C drive.

2.   Open the AUTODYN programme.

3.   Click on new.

    a.   Click on browse and search for the folder named Example.

    b.   Click on the Example folder.

    c.   Under Ident, name the model. We shall call the model Model_1.

    d.   Under Symmetry click 2D and Axial.

    e.   Under units click Length (cm), Mass (g) and Time (μs).

    f.   On completion click the "tick".

4.   Click on Material.

    a.   Click Load.

    b.   Select "Comp B" as Donor and click "tick".

    c.   Click Erosion.

    d.   Geometric Strain = 1.0.

    e.   Click Load.

f.   Select "Air" as the Gap materials and click "tick".

g.   Click Erosion.

h.   Geometric Strain = 1.0.

i.   Click Load.

j.   Select "CompBJJ3" as the Acceptor and click "tick".

k.   Click Erosion.

l.   Geometric Strain = 1.0.

5.   Click on Boundaries

     a.   Click New

     b.   Name the boundary. We shall call it Transmit.

     c.   Click Type and select "Transmit".

     d.   Click Preferred Material and select "ALL EQUAL".

     e.   On completion click the "tick".

6.   Click on Parts

     a.   Click New

           i.   Name the part Comp B.

           ii.   Select Lagrange and click "next".

           iii.   X origin = 0.0.

           iv.   Y origin = 0.0.

           v.   DX = 52.

           vi.   DY = 13.6.

           vii.   Click "next".

           viii.   Cells in I direction = 130.

           ix.   Cells in J direction = 34.

           x.   Click "next".

           xi.   Material select Comp B

           xii.   Click "tick".

     b.   Click New

           i.   Name the part Air Gap

           ii.   Select Lagrange and click "next".

       iii.   X origin = 52.0.

       iv.   Y origin = 0.0.

       v.   DX = 10.

       vi.   DY = 13.6.

       vii.   Click "next".

       viii.   Cells in I direction = 10.(@10 mm/cell)

       ix.   Cells in J direction = 14 (@10 mm/cell)

       x.   Click "next".

       xi.   Material select Air

       xii.   Int Energy = 1.0e-5

       xiii.   Click "tick".

c.   Click New

       i.   Name the part Comp BJJ3.

       ii.   Select Lagrange and click "next".

       iii.   X origin = 62.0

       iv.   Y origin = 0.0.

       v.   DX = 52.

       vi.   DY = 13.6.

       vii.   Click "next".

       viii.   Cells in I direction = 130.

       ix.   Cells in J direction = 34.

       x.   Click "next".

       xi.   Material select Comp BJJ3.

       xii.   Click "tick".

d.   Click Boundary

       i.   Select Comp B.

       ii.   Click I Line.

       iii.   I = 1.

       iv.   Click "tick".

       v.   Click J Line

vi.   J = 35.

vii.   Select Air Gap.

viii.   Click J Line.

ix.   J = 15.

x.   Select Comp BJJ3.

xi.   Click I Line.

xii.   I = 131.

xiii.   Click "tick".

xiv.   Click J Line

xv.   J = 35.

e.   Click Gauges

    i.   Select Comp B.

    ii.   Click "Add".

    iii.   Click "Array".

    iv.   Click "Fixed"

    v.   Click "XT-Space".

    vi.   Click "X-Array".

    vii.   X min = 0.0

    viii. X max = 52.0

    ix.   X increment = 4.0

    x.   Y co-ordinate = 0.0

    xi.   Select Comp BJJ3.

    xii.   Click "Add".

    xiii.   Click "Array".

    xiv.   Click "Fixed"

    xv.   Click "XT-Space".

    xvi.   Click "X-Array".

    xvii. X min = 62.0

    xviii. X max = 114.0

    xix.   X increment = 4.0

xx.   Y co-ordinate = 0.0

xxi.   Click Review (to see the gauge co-ordinates).

f.   Select Air Gap

i.   Click "Zoning".

ii.   Click "Transformation".

iii.   Click "Translate".

iv.   DX = 0.12.

v.   DY = 0.0.

vi.   Click "tick".

g.   Select Comp BJJ3

i.   Click "Zoning".

ii.   Click "Transformation".

iii.   Click "Translate".

iv.   DX = 0.24.

v.   DY = 0.0.

vi.   Click "tick".

h.   Click Gauges

i.   Click "Review" (to see the new gauge co-ordinates).

i.   Click Detonation

i.   Click "Line".

ii.   X1 = 0.0.

iii.   Y1 = 0.0.

iv.   X2 = 0.0.

v.   Y2 = 13.6.

vi.   Path = indirect.

j.   Click Conrol

i.   Cycle Limit = 100 000.

ii.   Time limit = 100 000.

k.   Click Output

i.   Start Cycle = 0.

    ii. End Cycle = 100 000.

    iii. Increment = 100.

 L. Click Save.

 M. Click Run.

APPENDIX F   MATERIAL PROPERTIES

The AUTODYN code was used for the simulation studies and the material properties for the respective components are detailed below.

1. **Composition B**

Density		1.717g/cm^3
JWL Reacted EOS		
	A	5.2423Mbar
	B	0.07678Mbar
	R1	4.2
	R2	1.1
	W	0.34
C-J	Detonation Velocity	$0.798 \text{cm}/\mu \text{s}$
C-J	Energy/unit volume	0.085Gerg/mm^3
C-J	Pressure	0.295Mbar
Erosion Model		Geometric Strain
	Erosion Strain	1.0
	Type of Geometric Strain	Instantaneous

2. **Composition B JJ3**

Density		1.717g/cm^3
JWL Reacted EOS		
	A	5.2423Mbar
	B	0.07678Mbar
	R1	4.2
	R2	1.1
	W	0.34
C-J	Detonation Velocity	$0.798 \text{cm}/\mu \text{s}$
C-J	Energy/unit volume	0.085Gerg/mm^3
C-J	Pressure	0.295Mbar
Reaction zone width		2.5
Max change in reaction ratio		0.1
Ignition parameter I		4.0×10^6
Ignition reaction ratio exp.		0.667
Ignition compression exp.		7.0
Growth parameter G1		850
Growth reaction ratio exp.c		0.222
Growth reaction ratio exp.d		0.667
Growth reaction ratio exp.y		2.0
Growth parameter G2		660.0

Growth reaction ratio exp.e	0.333	
Growth reaction ratio exp.g	1.0	
Growth pressure exp.z	3.0	
Max. reac. ratio: ignition	0.022	
Max reac. ratio: growth G1	0.60	
Min. reac. ratio growth G2	0.0	
Maximum rel. vol in tension	1.1	

JWL Unrreacted EOS

A	778.09976Mbar
B	-0.05031Mbar
R1	11.3
R2	1.13
W	0.8938
Von Neumann spike rel vol	0.6933
C-J Energy/unit volume	-0.006120

Strength Model	Von Misses
Shear Modulus	0.035Mbar
Yield Stress	0.002Mbar

Erosion Model	Geometric Strain
Erosion Strain	1.0
Type of Geometric Strain	Instantaneous

3. Air

Density 0.001225g/cm^3

EOS	Ideal Gas
Gamma	1.4
Adiabatic constant	0.0
Pressure shift	0.0
Reference Temperature	282.2K
Specific Heat	$7.176 \times 10^{-6}\text{Terg/gK}$

Erosion Model	Geometric Strain
Erosion Strain	1.0
Type of Geometric Strain	Instantaneous

4. Plexiglas

Density 1.186g/cm^3

EOS	Shock
Guneisen coefficient	0.97
Parameter C1	$0.2598 \text{cm}/\mu \text{s}$

Parameter S1   1.516

Erosion Model   Geometric Strain
    Erosion Strain   1.0
    Type of Geometric Strain   Instantaneous

5.   **Teflon**
Density 2.153g/cm^3

EOS   Shock
    Guneisen coefficient   0.59
    Parameter C1 $0.1841 \text{cm}/\mu \text{s}$
    Parameter S1   1.707

Erosion Model   Geometric Strain
    Erosion Strain   1.0
    Type of Geometric Strain   Instantaneous

THIS PAGE INTENTIONALLY LEFT BLANK

LIST OF REFERENCES

1. Cooper ,P. W., Explosive Engineering, Wiley-VCH Inc,1996.

2. Kubota, S. , Zhiyue, L. , Otsuki, M. , Nakayama, Y. , Ogata, Y. and Yoshida, M. Material Science Forum Vols 456-466 (2004) pp. 163-168. A Numerical Study of Sympathetic Detonation in Gap Test.

3. Eaton, P. E. , Zhang, M. X. , Gilardi, R. , Gelber, N. , Iyer, S. , Rao, S. Propellant, Explosives, Pyrotechnics 27, 1-6 (2002). Octanitrocubane: A New Nitrocarbon.

4. Philibin, S. P. Millar, R. W. and Coombes, R. G. Propellant, Explosives, Pyrotechnics 25, 302-306 (2000). Preparation of 2,5-Diamino-3,6-Dinitropyrazine (ANPZ-i): A Novel Candidate High Energy Insensitive Explosive.

5. Li, J. and Dong, H. Propellant, Explosives, Pyrotechnics 29, (2004) No 4. Theoretical Calculation and Molecular Design for High Explosives: Theoretical Study on Polynitropyrazines and their N-oxides.

6. Sleadd, B. A. and Clark, G. 2004 Insensitive Munitions and Energetic Materials Technology Symposium. Improved Synthesis of a Precursor for Reduced-Sensitivity RDX (RS-RDX).

7. Dahlberg, J. and Sjoberg, P. 2004 Insensitive Munitions and Energetic Materials Technology Symposium. FOX-7 and its Application.

8. Swanson, R. L. 2004 Insensitive Munitions and Energetic Materials Technology Symposium. Aging of Insensitive Munitions, A Navy Quality Evaluation Perspective.

9. Maienschein, J. L. Energetic Materials Centre, Lawrence Livermore National Laboratory. Qualification of Insensitive High Explosive Using Modern Testing and Analysis.

10. Desailly, D. Chabin, P. ,Lecume, S. and Freche, A. 2004 Insensitive Munitions and Energetic Materials Technology Symposium. New Concept to Prevent Sympathetic Detonation

11. Phua, T.C. Naval Postgraduate School. Quantitative Code Evaluation for Predicting Shaped Charge and Characteristics, Thesis (2003).

12. Century Dynamics Inc. Interactive Non-Linear Dynamic Analysis Software. AUTODYN Introductory Training Course July 2005.

13. Century Dynamics Inc. Interactive Non-Linear Dynamic Analysis Software AUTODYN 2D V5, Explosive Library Menu.

14.   Century Dynamics Inc. AUTODYN Interactive Non-Linear Dynamic Analysis Software, Explosive Initiation Users Manual (Lee-Tarver Ignition and Growth) Revision 4.3.

15.   Miller, P. and Alexander, K., "Determining JWL Equation of State Parameters Using the Gurney Equation Approximation", Proceedings of the Ninth (Int'l) Detonation Symposium, Portland OR, Sep. 1989.

16.   Baker, E.L and Stiel, L.I, "Optimized JCZ3 Procedures for the Detonation Properties of Explosives. Proceedings of the Eleventh (Int'l) Detonation Symposium, Snowmass, CO, Sep. 1998.

INITIAL DISTRIBUTION LIST

1.   Defense Technical Information Center
        Ft. Belvoir, Virginia

2.   Dudley Knox Library
        Naval Postgraduate School
        Monterey, California

3.   Professor Anthony J. Healy
        Naval Postgraduate School
        Monterey, California

4.   Professor Jose O. Sinibaldi
        Naval Postgraduate School
        Monterey, California

5.   Professor Ronald E. Brown
        Naval Postgraduate School
        Monterey, California

6.   Professor Yeo Tat Soon
        Director, Temasek Defense Systems Institute
        Singapore

7.   Mdm Tan Lai Poh
        Temasek Defense Systems Institute
        Singapore

8.   Defence Science & Technology Agency
        Human Resource Department
        Singapore

9.   Dr Chris X. Quan
        Century Dynamics Incorporated
        Concord, California